



HAL
open science

Fluxnet and regional carbon flux modeling, spatial integration and regional fluxes, spatial scales of coherence, network-scale analysis

Philippe Ciais, Markus Reichstein, Kenneth Davis, Toshinobu Machida, Dario Papale, Galina Churkina, Scott Denning, Gen Inoue, Ivan Janssens, Natasha Miles, et al.

► To cite this version:

Philippe Ciais, Markus Reichstein, Kenneth Davis, Toshinobu Machida, Dario Papale, et al.. Fluxnet and regional carbon flux modeling, spatial integration and regional fluxes, spatial scales of coherence, network-scale analysis. FLUXNET Workshop "Celebrating 10 years Since La Thuile and Planning for the Future", Dec 2004, Firenze, Italy. 58 pl. hal-01189430

HAL Id: hal-01189430

<https://hal.science/hal-01189430>

Submitted on 7 Jun 2020

HAL is a multi-disciplinary open access archive for the deposit and dissemination of scientific research documents, whether they are published or not. The documents may come from teaching and research institutions in France or abroad, or from public or private research centers.

L'archive ouverte pluridisciplinaire **HAL**, est destinée au dépôt et à la diffusion de documents scientifiques de niveau recherche, publiés ou non, émanant des établissements d'enseignement et de recherche français ou étrangers, des laboratoires publics ou privés.

Fluxnet and regional carbon flux modeling

(spatial integration and regional fluxes, spatial scales of coherence, network-scale analysis),

Ph. Ciais, M. Reichstein, K. Davis, T. Machida, D. Papale, S. Arshimov, G. Churkina, S. Denning, G. Inoue, I. Janssens, N. Miles, S. Richardson, K. Trusilova, R. Valentini, N. Viovy, A. Granier ⁽⁴⁾, J. Ogée ⁽⁵⁾, V. Allard ⁽⁶⁾, M. Aubinet ⁽⁷⁾, Chr. Bernhofer ⁽⁸⁾, A. Carrara ⁽⁹⁾, F. Chevallier ⁽¹⁾, N. De Noblet ⁽¹⁾, A. Friend ⁽¹⁾, T. Grünwald ⁽⁸⁾, B. Heinesch ⁽⁷⁾, P. Keronen ⁽¹⁰⁾, A. Knohl ^(11,12), D. Loustau ⁽⁵⁾, G. Manca ⁽²⁾, G. Matteucci ⁽¹³⁾, F. Miglietta ⁽¹⁴⁾, J.M. Ourcival ⁽¹⁵⁾, K. Pilegaard ⁽¹⁶⁾, S. Rambal ⁽¹⁵⁾, G. Seufert ⁽¹³⁾, J.-F. Soussana ⁽⁶⁾, M.-J. Sanz ⁽⁹⁾, E.D. Schulze ⁽¹¹⁾, T. Vesala ⁽¹⁰⁾

Estimating regional fluxes

Atmospheric
inversions

Ill posed problem
Errors amplification

Completeness
Not traceable to processes

Downscaling

Upscaling

Hétérogénéities
Variability

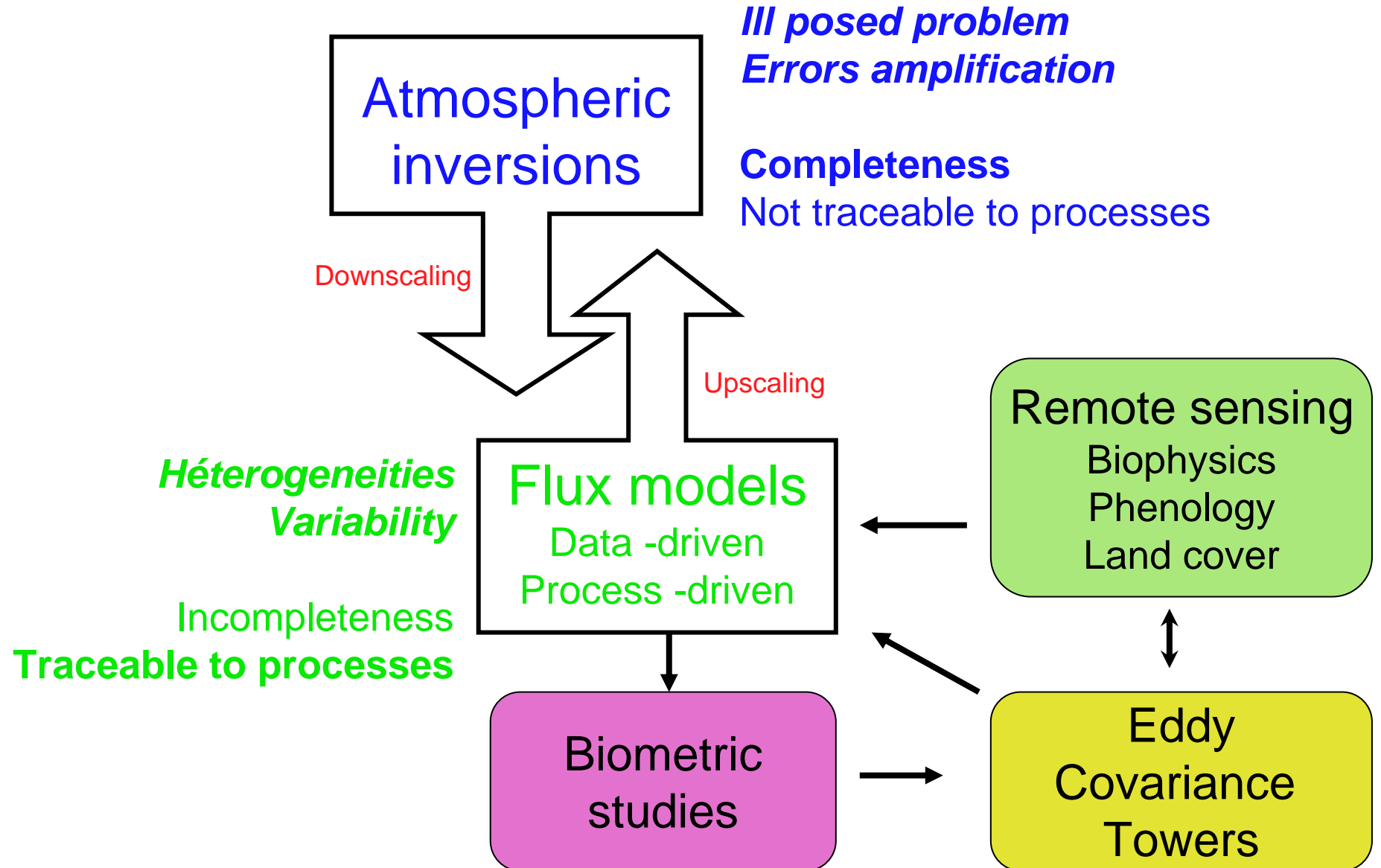
Flux models
Data -driven
Process -driven

Remote sensing
Biophysics
Phenology
Land cover

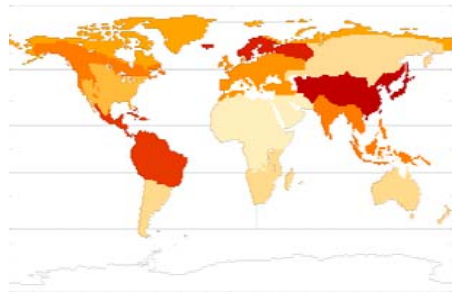
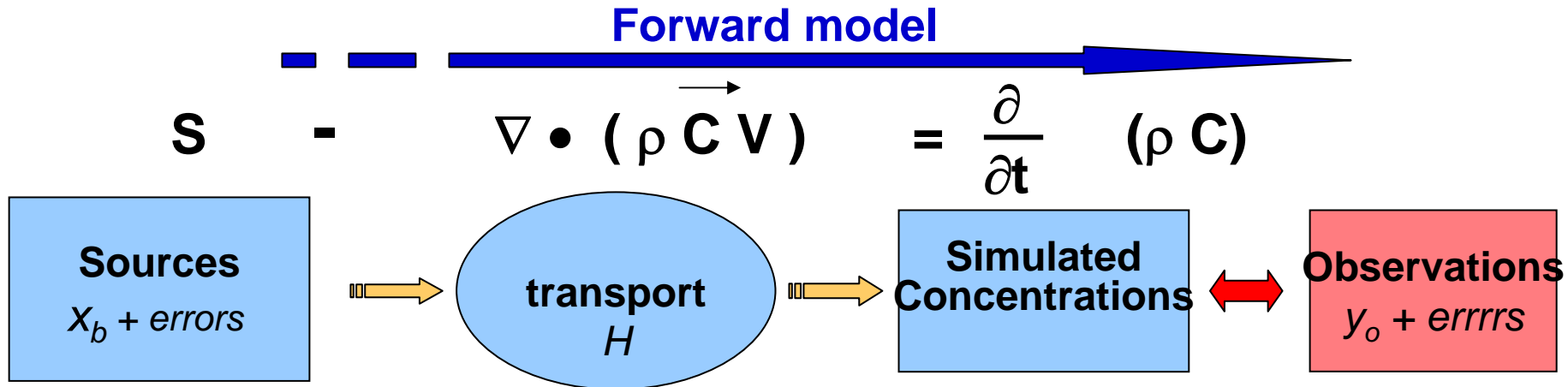
Incompleteness
Traceable to processes

Biometric
studies

Eddy
Covariance
Towers

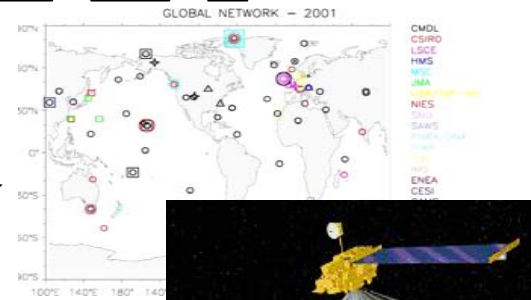


Inversions



Inversion

$$\mathbf{H} \mathbf{x} = \mathbf{y}$$

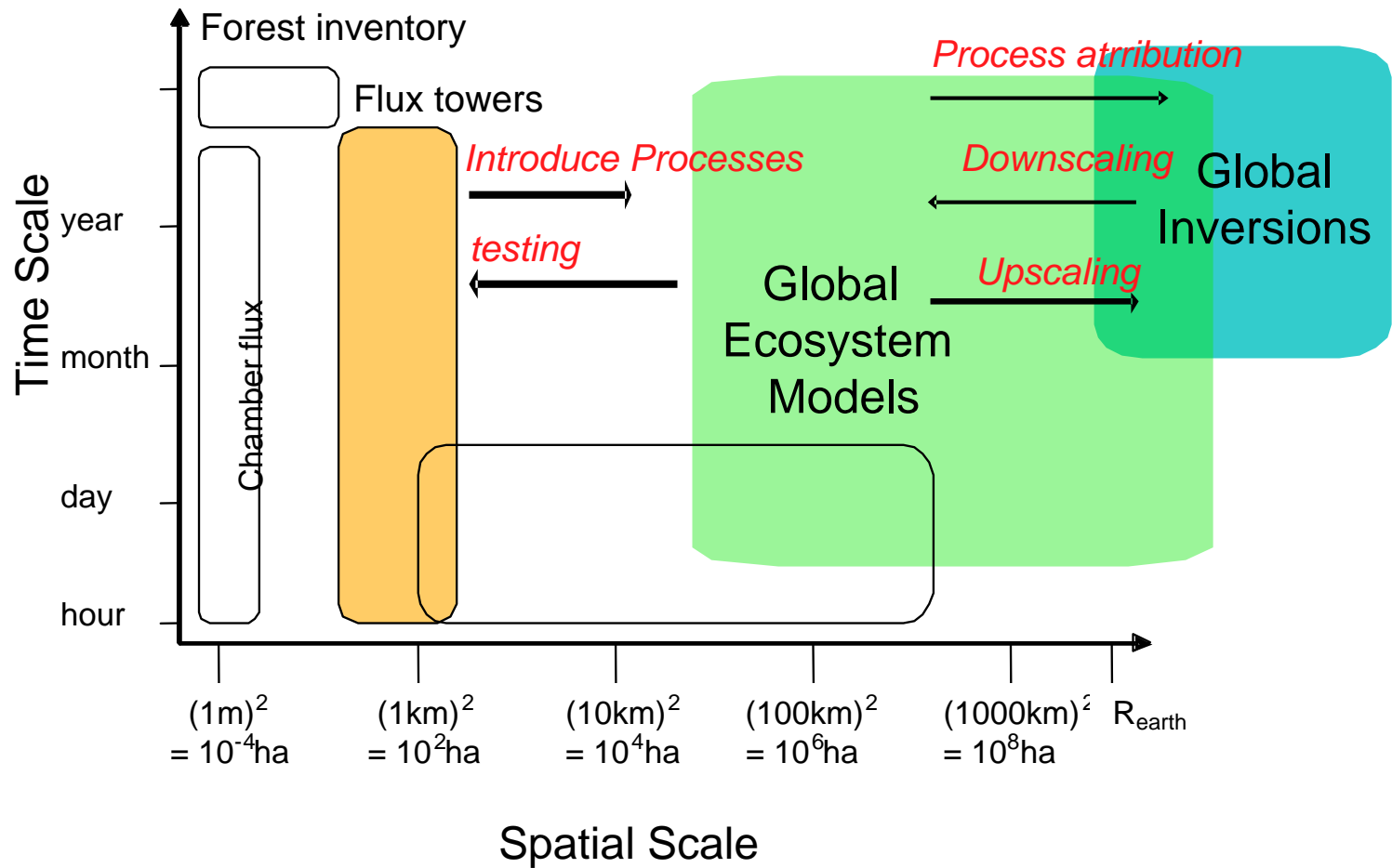


Flux estimate x_a which produces the best fit the atmospheric data

Estimation : $x_a = x_b + (\mathbf{H}^T \mathbf{R}^{-1} \mathbf{H} + \mathbf{P}^{-1})^{-1} \mathbf{H}^T \mathbf{R}^{-1} (\mathbf{y}_0 - \mathbf{H} x_b)$

Error : $\mathbf{P}_a = (\mathbf{H}^T \mathbf{R}^{-1} \mathbf{H} + \mathbf{P}^{-1})^{-1}$

Joint constraints! Complementary methods : 1. Continental budgets

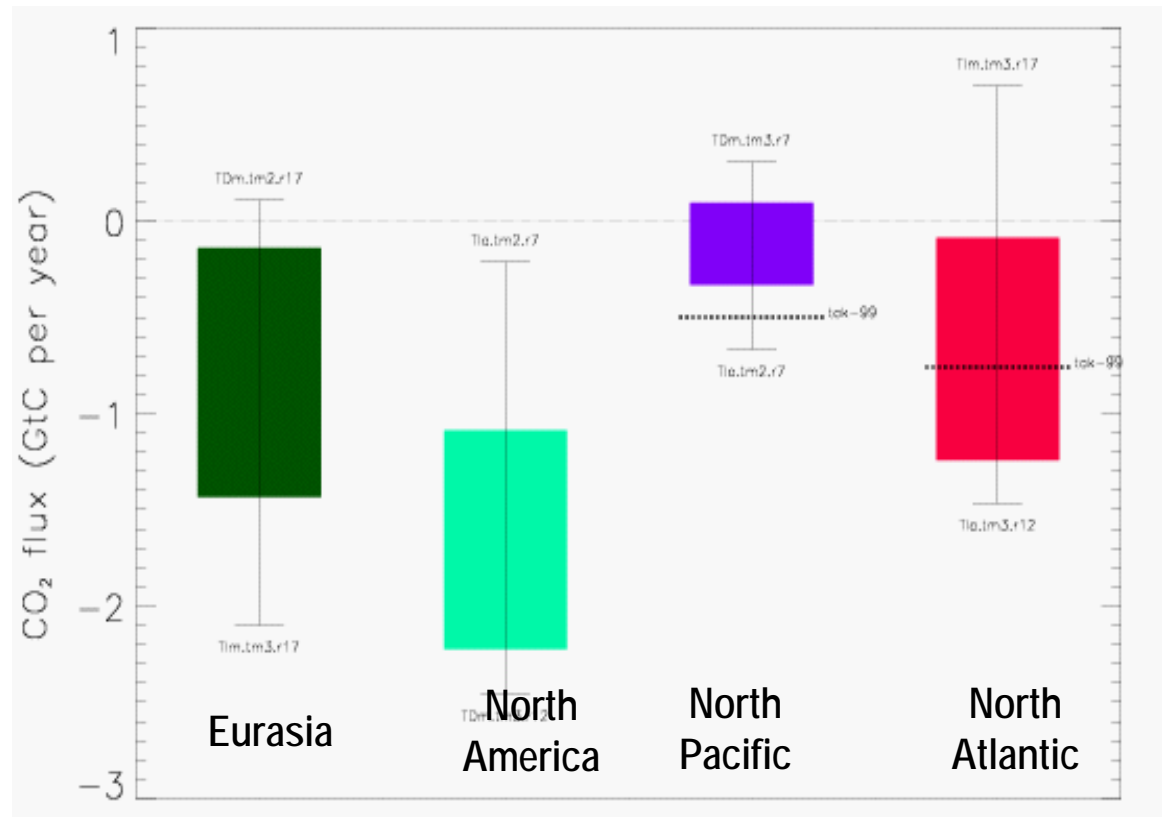


Inversion of Continental Fluxes

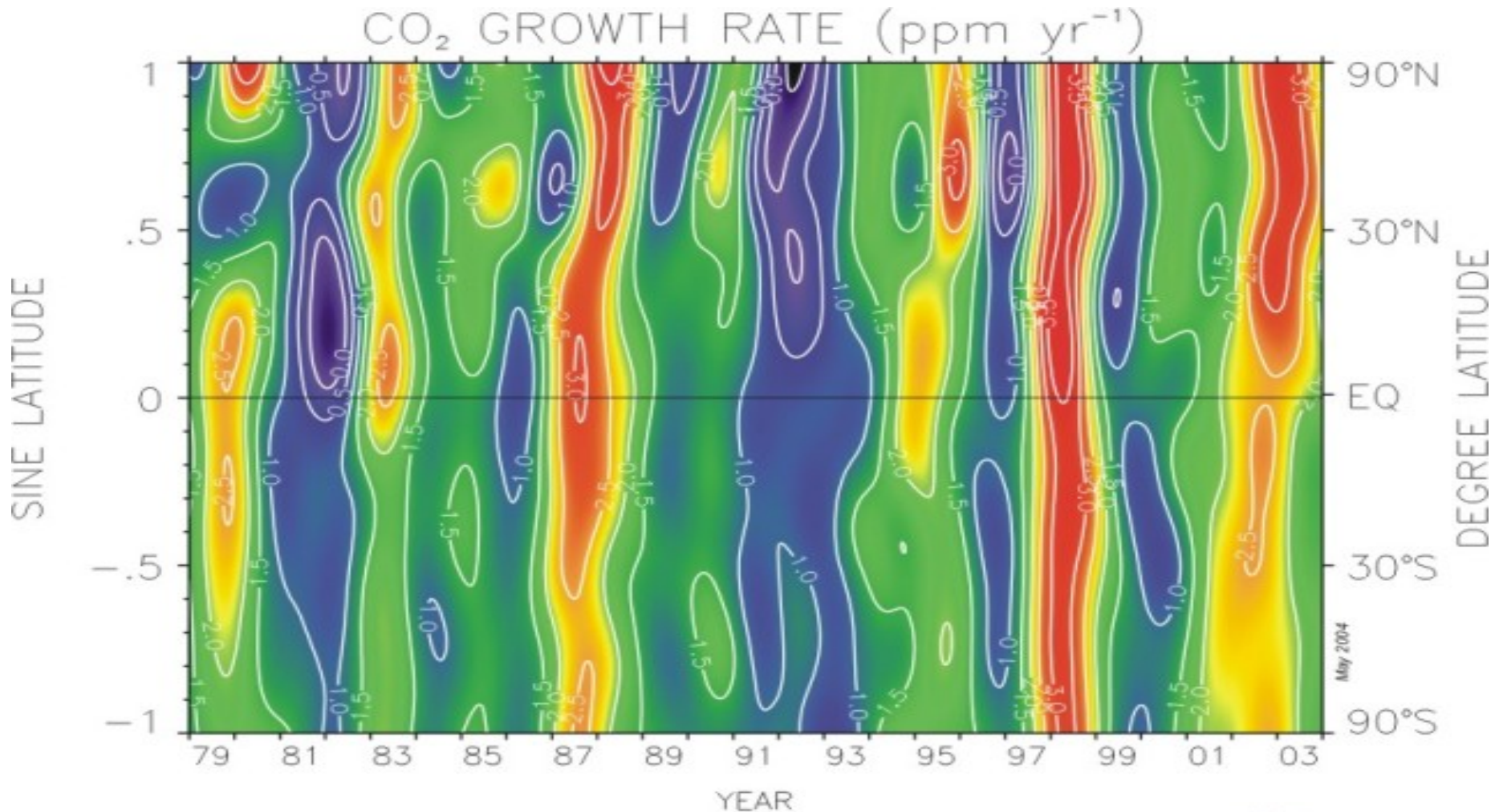
Apportionment of NH sink in longitude

Sources of uncertainties

- Data errors
- Network density
- Transport biases
 - seasonal vertical advection*
- Inversion set-up
 - Prior flux aggregations*
 - Prior errors*
 - Prior estimate*



Interannual variations in CO₂ growth rate



Contour plot showing the temporal and spatial variations in the atmospheric increases of carbon dioxide. The cooler colors (green, blue, violet) represent periods of lower than average growth rates and the warmer colors (yellow, orange, red) represent high growth rate periods. The plot is derived from measurements of thousands of samples collected at the CMDL cooperative air sampling network sites. The variations in the growth rate of this climatically important gas are due to interannual variations in the imbalance between sources and sinks, and also to variations in atmospheric transport. Principal investigator: Thomas Conway, NOAA CMDL Carbon Cycle Greenhouse Gases, Boulder, Colorado, (303)497-6681 (thomas.j.conway@noaa.gov, <http://www.cmdl.noaa.gov/ccgg>).

IAV of global fluxes

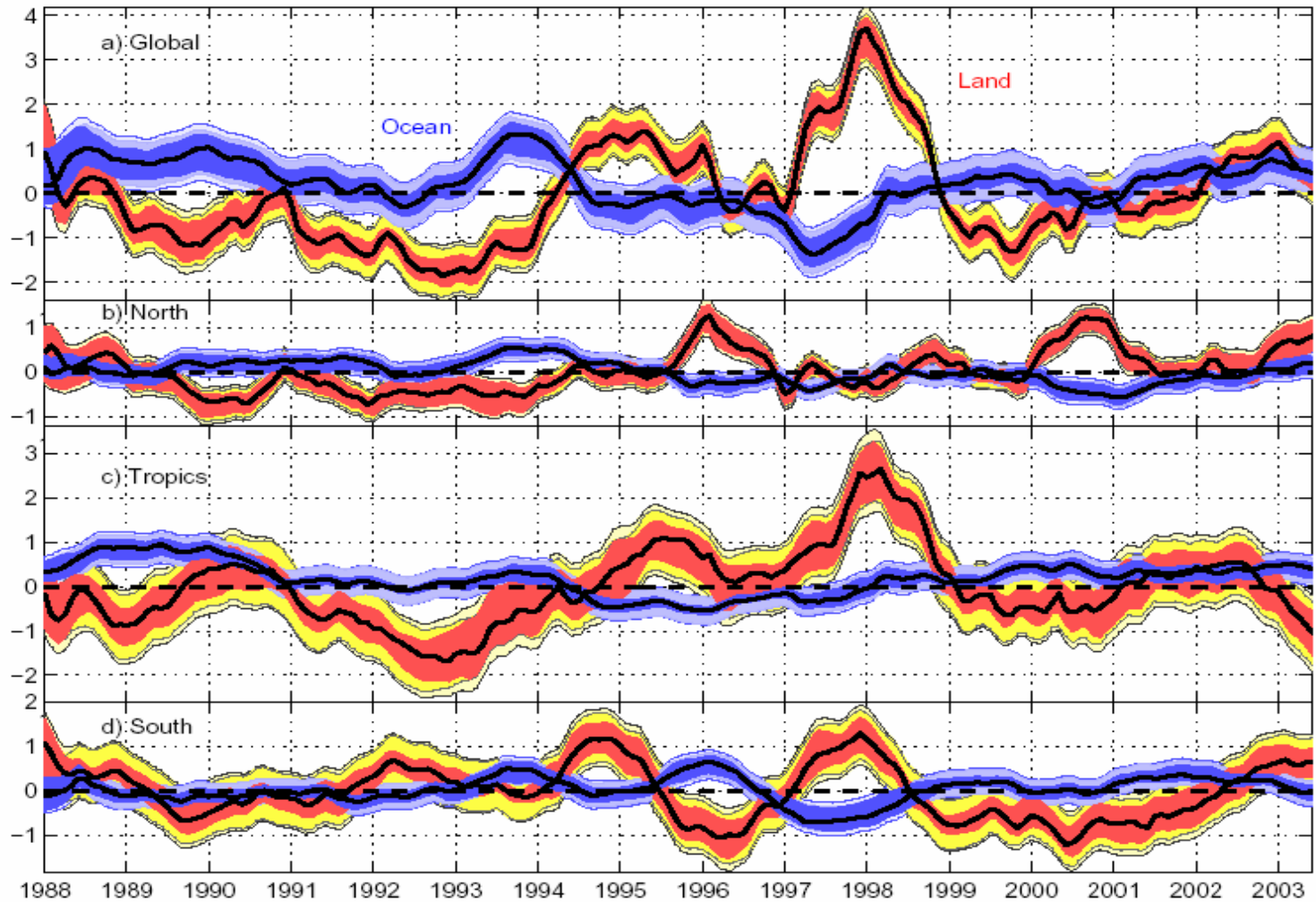


Figure 4. The land and ocean flux interannual variability (PgC yr^{-1}) from x^{IAV} for the full globe, and for the three broad latitude bands defined in Table 4.

IAV of Continental scale fluxes

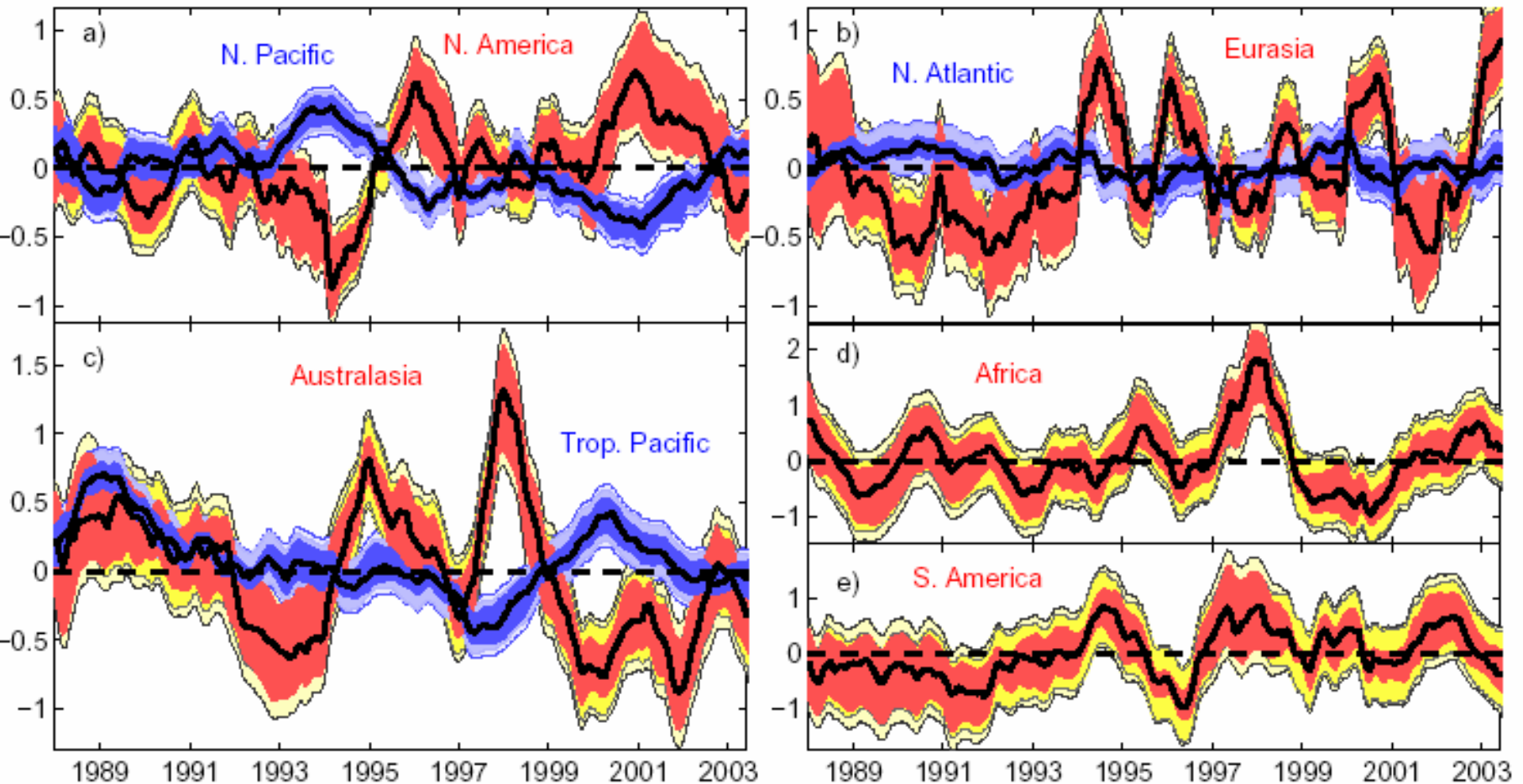
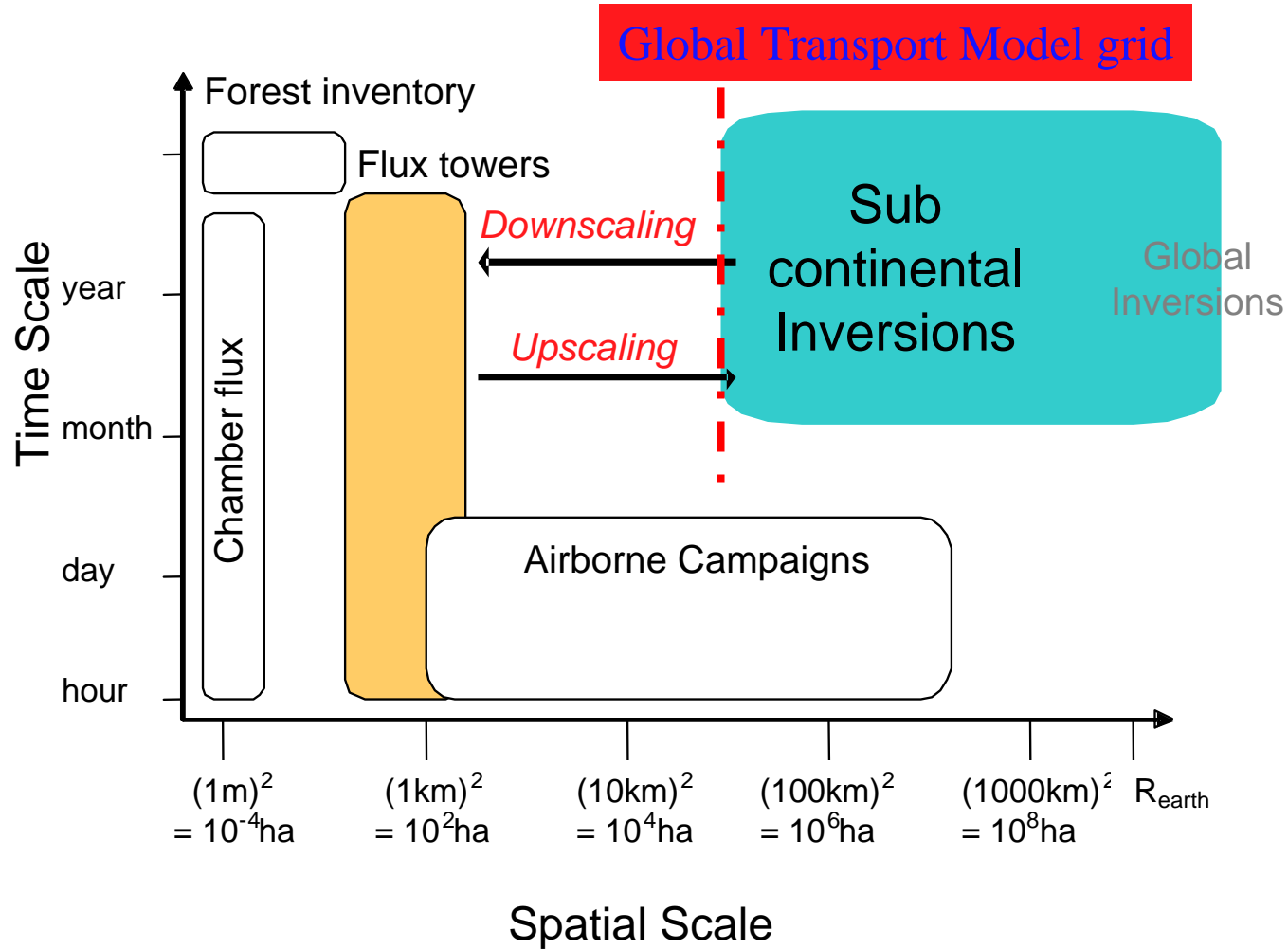


Figure 5. The 13-model mean CO₂ flux IAV [PgC yr⁻¹] from x^{IAV} on the continent/basin scale for the regions defined in Table 4: a) North Pacific & North America, b) North Atlantic & Eurasia, c) Australasia & Tropical Pacific, d) Africa, and e) South America (note the different scales for Africa and S. America).

Joint constraints! Complementary methods : 2. sub-continental budgets



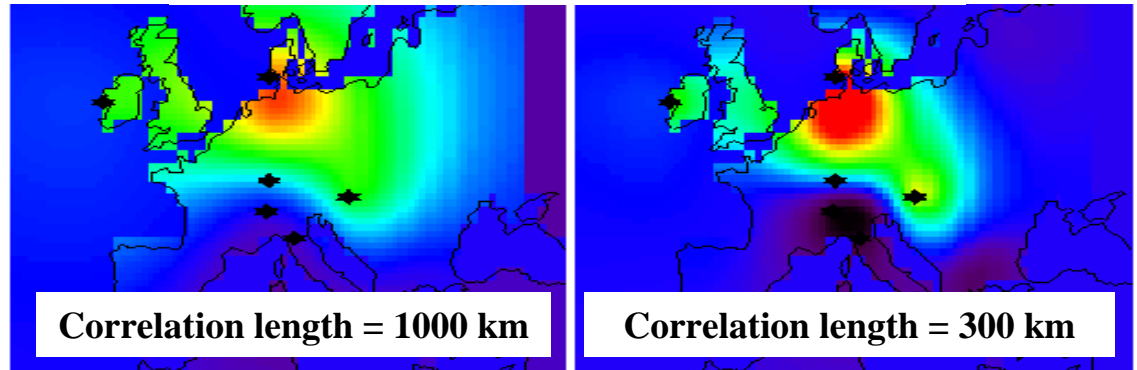
Inversions on the model grid

Regional scale Fluxes

from continuous CO₂ concentrations

Daily fluxes over Europe at 50 km
(over the rest of globe (large regions))

Flux correction



Sources of Uncertainty

- Transport

Synoptic horizontal

Diurnal vertical

- Prior Fluxes

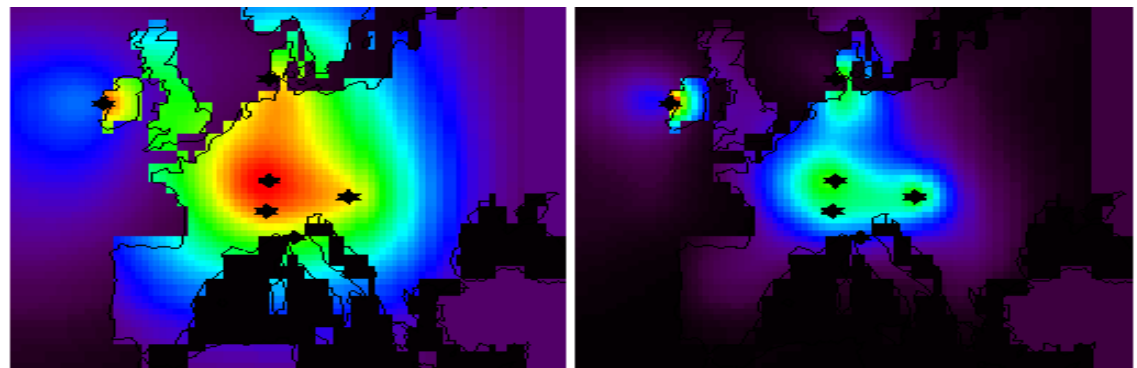
Scales of coherence

Diurnal Cycle

Synoptic variability

- Representiveness

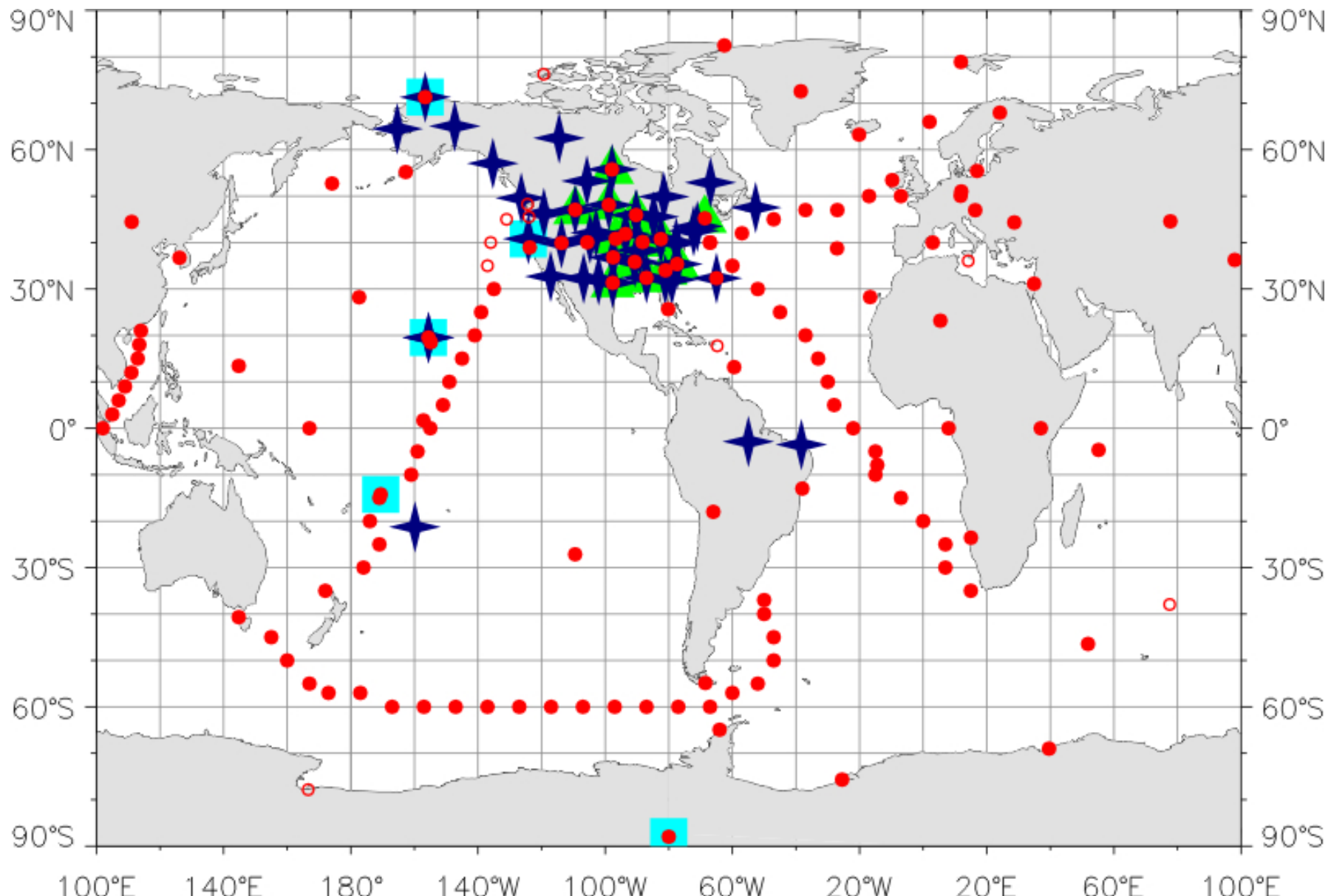
- Network density



5% Error Reduction from Prior (%) 50%

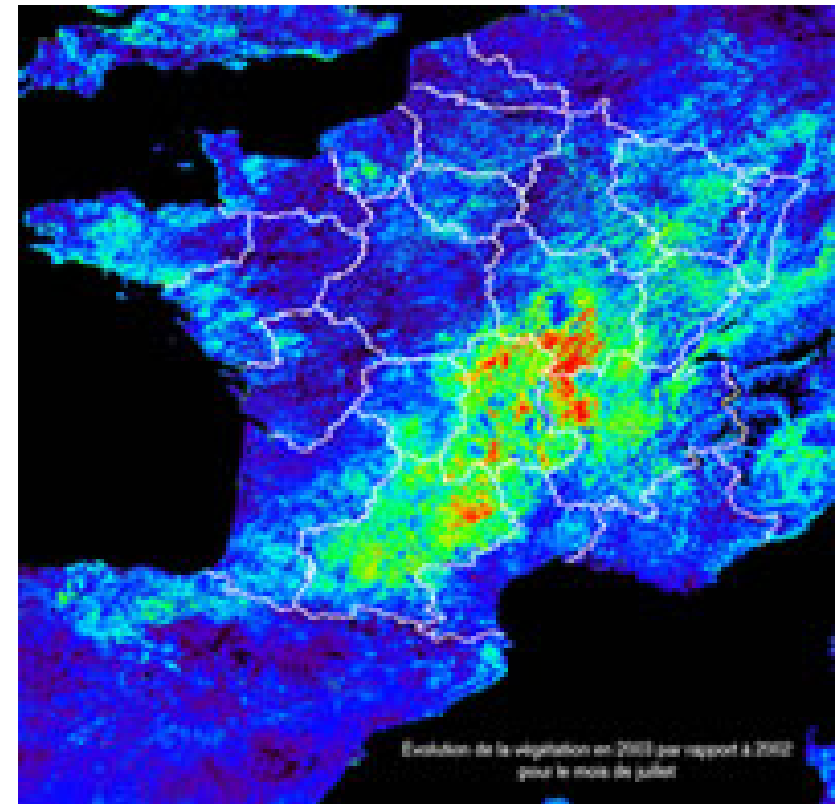
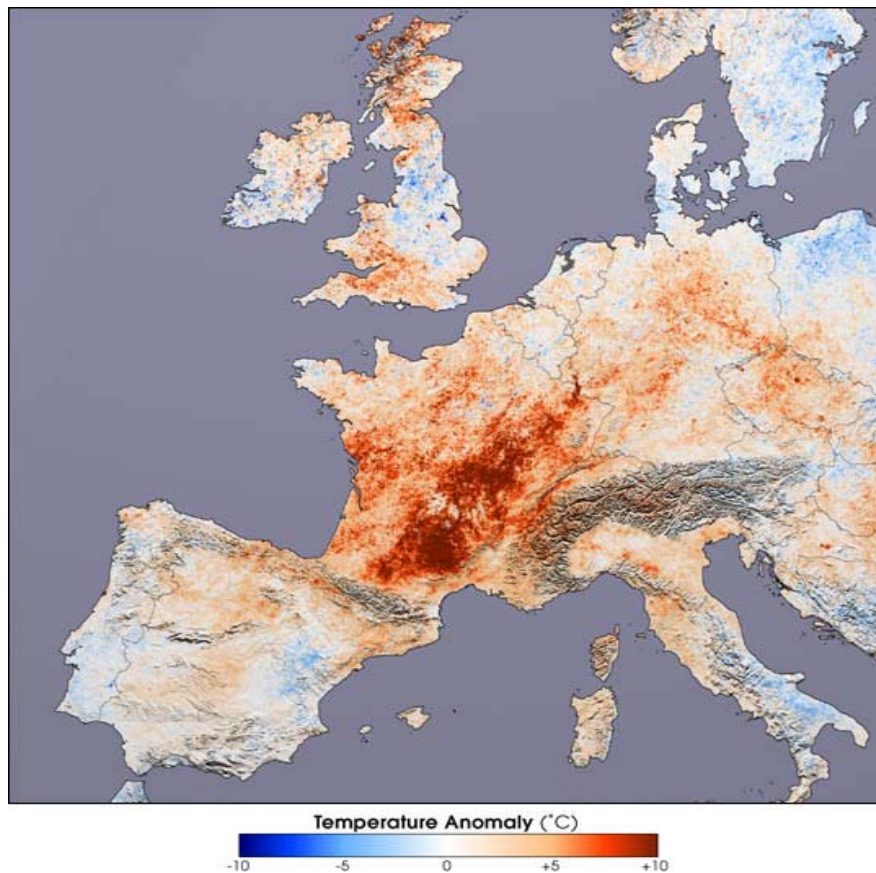
Carouge et al. 2004

NOAA CMDL Carbon Cycle Greenhouse Gases MEASUREMENT PROGRAMS - 2007



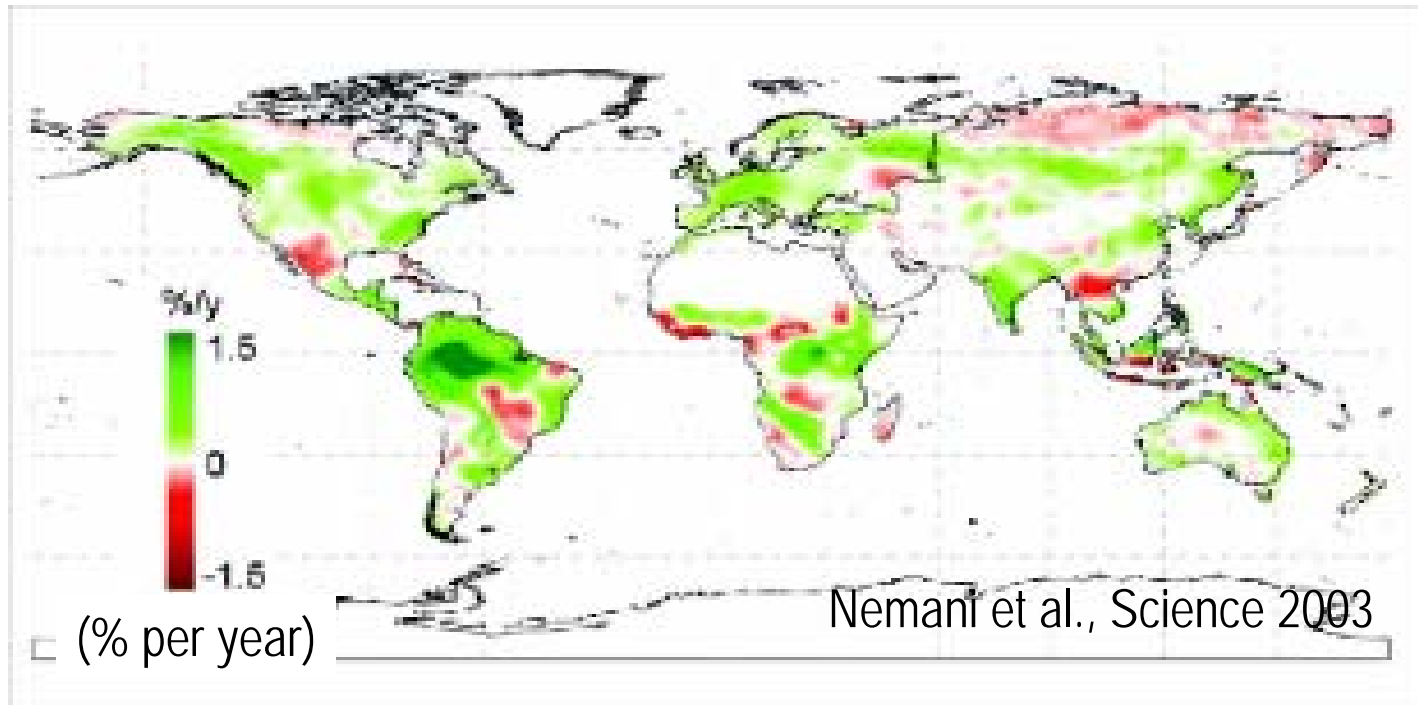
Linking bottom up observations ?

A 2003 European heatwave case study



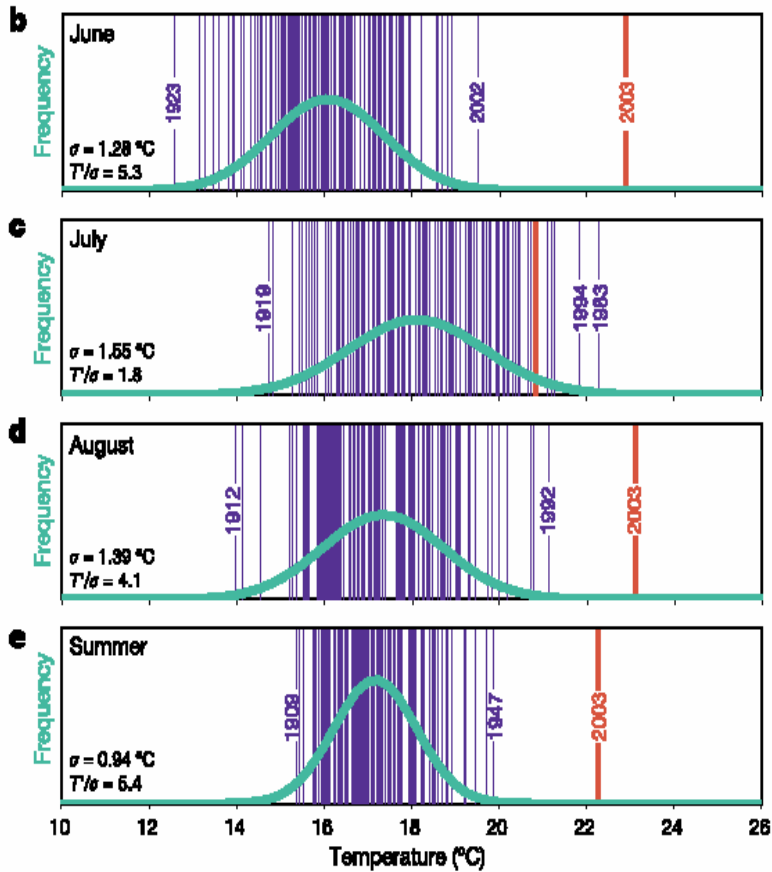


Secular increase in primary productivity from satellite NDVI over the past 25 years



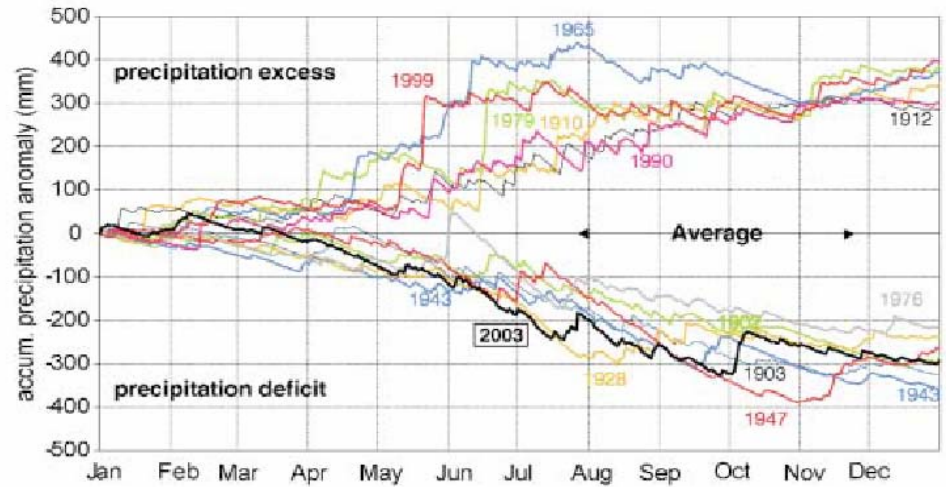
Will the greening continue if more frequent climate extremes impact productivity and net fluxes ?

Historical temperature records in Switzerland

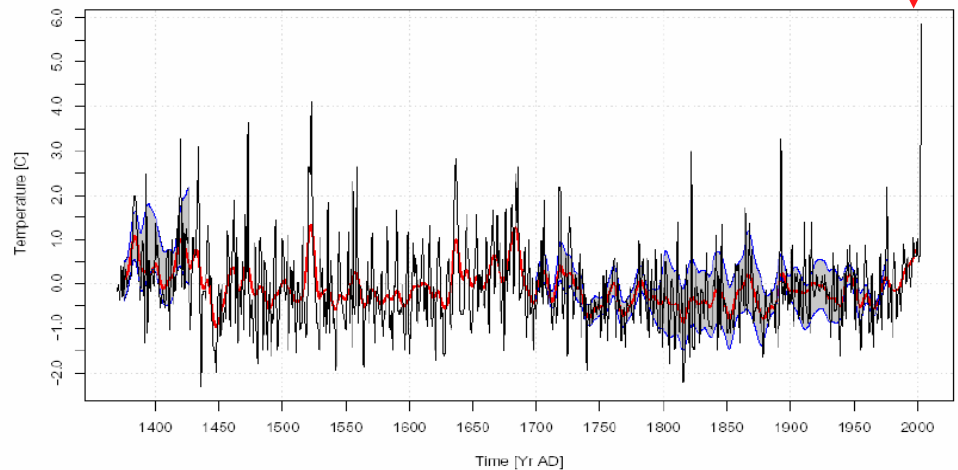


Shär et al., Nature 2003

Precipitation history in Bavaria



Summer temperature reconstruction from harvest dates in Burgundy



Chuine et al., Nature, 2004

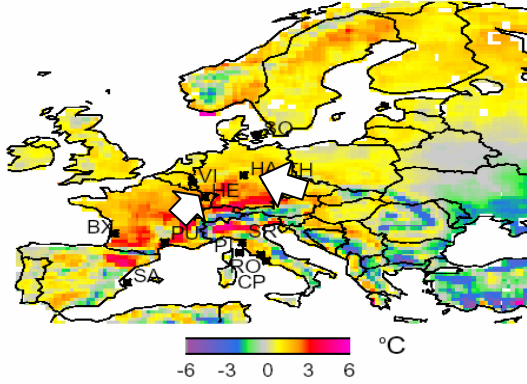
Integrating Regional Carbon Budgets

- Eddy covariance fluxes
- Crop yield statistics
- Remote sensing
- Atmospheric concentration
- Tree rings
- Terrestrial ecosystem models

Multiple Constraint Observations

	Spatial representativity	Temporal resolution	Information on processes	Long term record
Flux Towers Network	-- (++ from processes and network)	+++	+++	-
Crop yields	+ Averaged at the resolution of yield data	--	---	+++
Remote sensing	+++ But only GPP, NPP	+++ But only GPP, NPP	-	+ From different sensors

JUL-SEP Temperature 2003 vs 1998-2002



Two Beech forests

Hainich

Eastern Germany

150 years

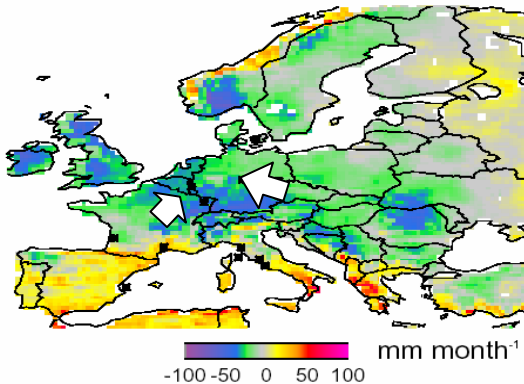
Hesse

Eastern France

30 yrs

QuickTime™ et un
décompresseur TIFF (LZW)
sont requis pour visionner cette image.

Annual Rain 2003 vs 1998-2002



Mediterranean forests

Holm oak

Maquia

Oak

Pine

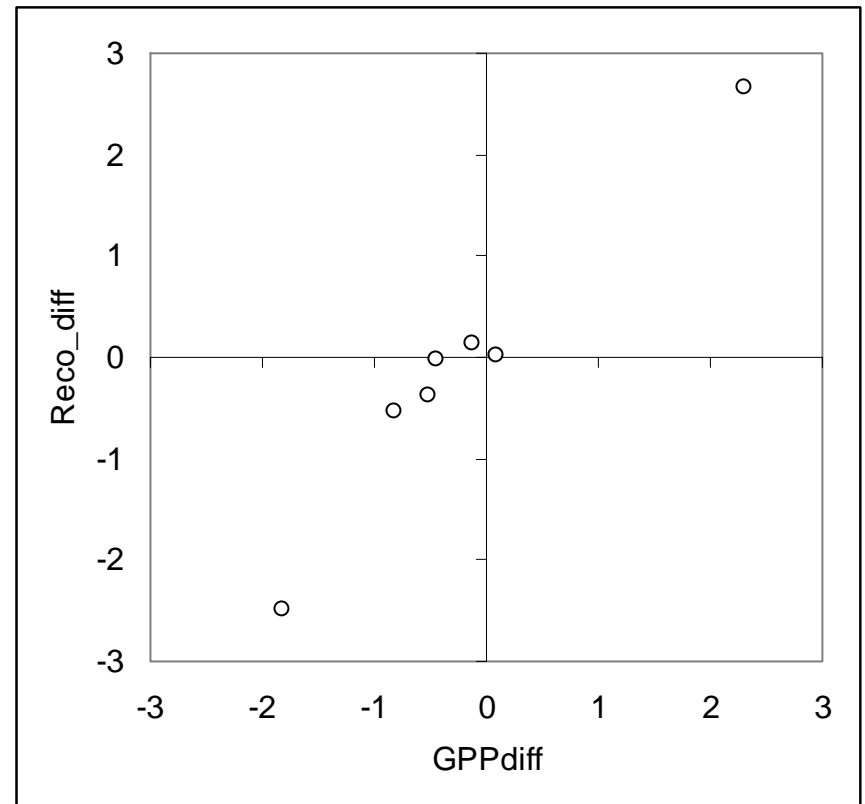
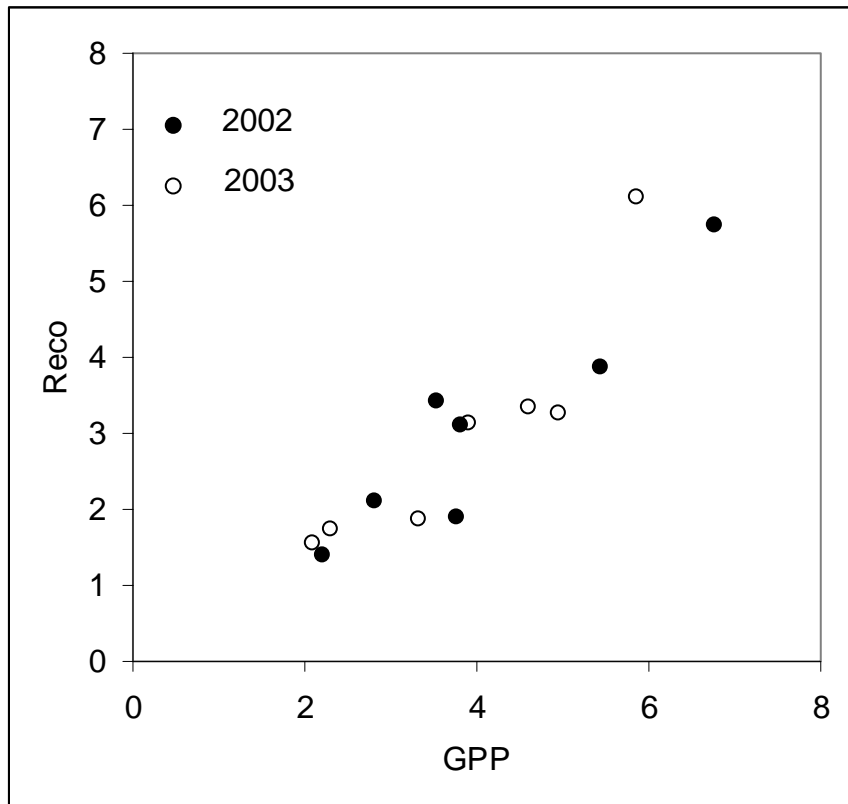
QuickTime™ et un
décompresseur TIFF (LZW)
sont requis pour visionner cette image.

QuickTime™ et un
décompresseur TIFF (LZW)
sont requis pour visionner cette image.

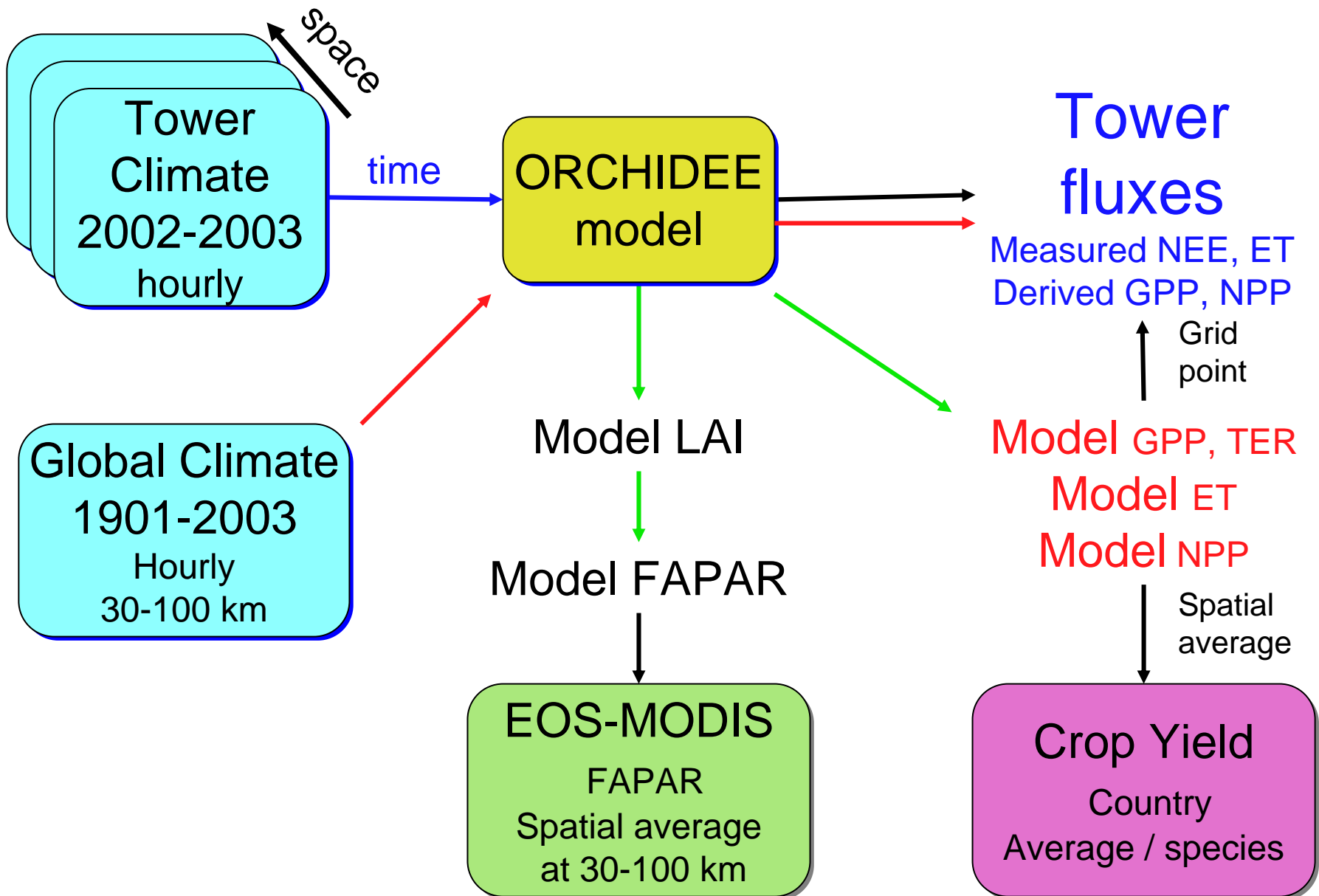
Annual GPP and TER ...

are coupled...

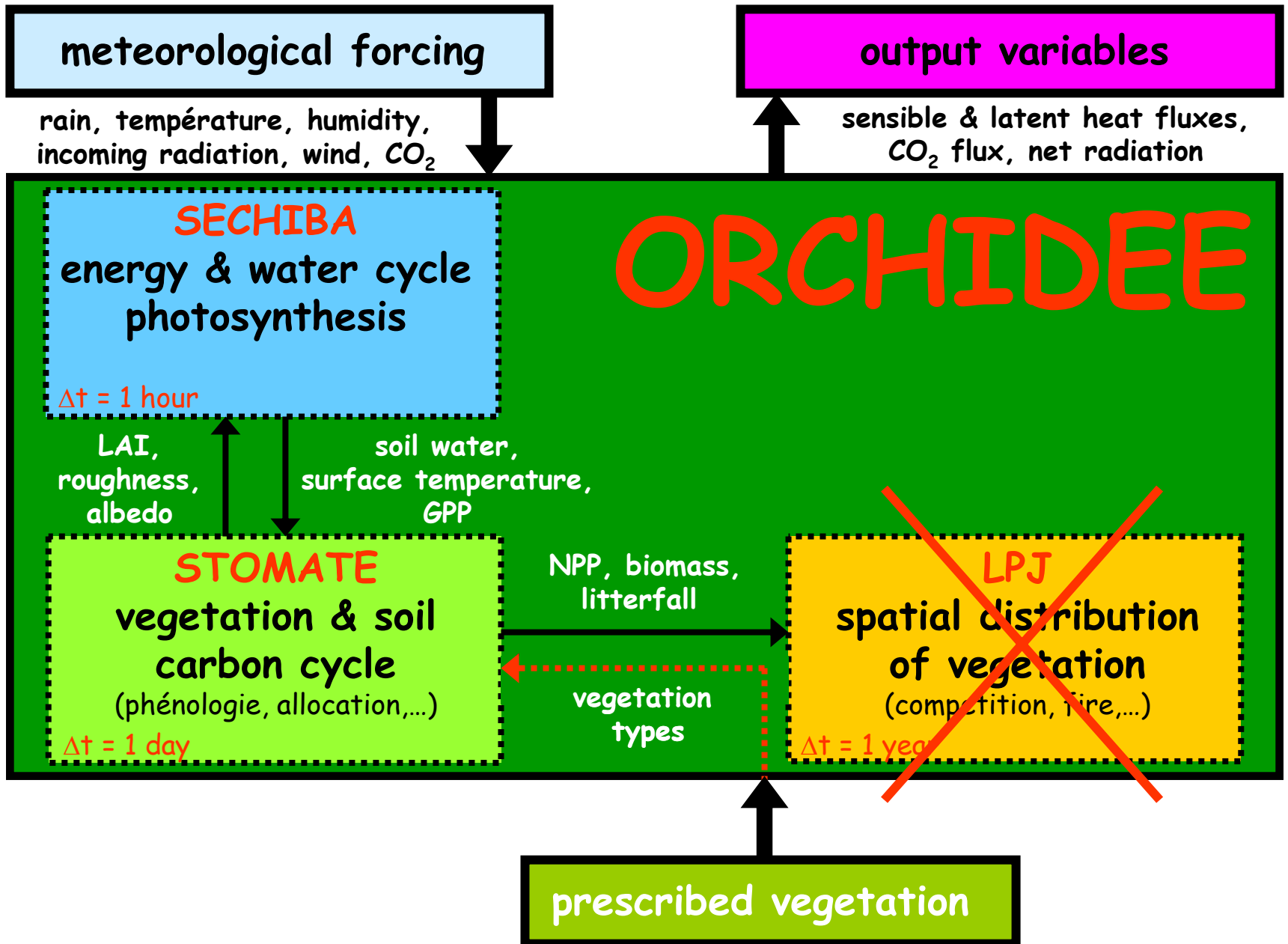
... and even the difference 2003-2002.



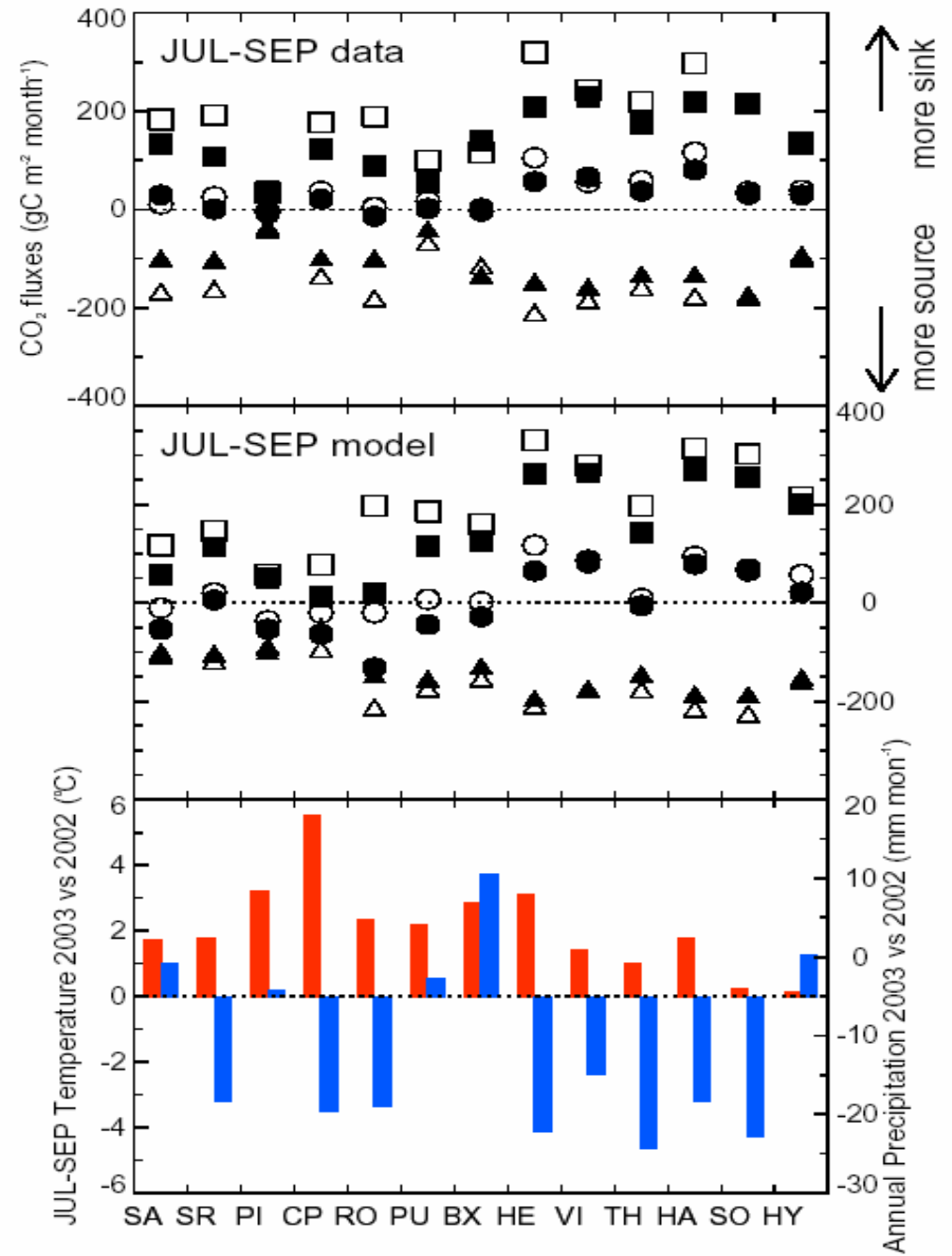
2003 modelling system



Global biospheric model ORCHIDEE



Gross and net fluxes in 2002 and 2003



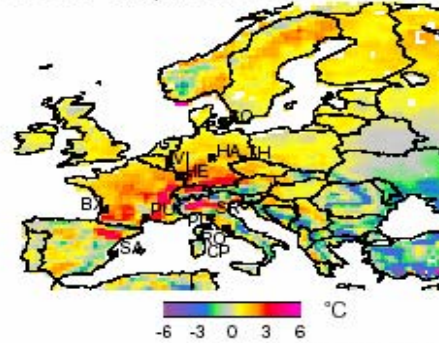
Abnormal Climate and Productivity in 2003



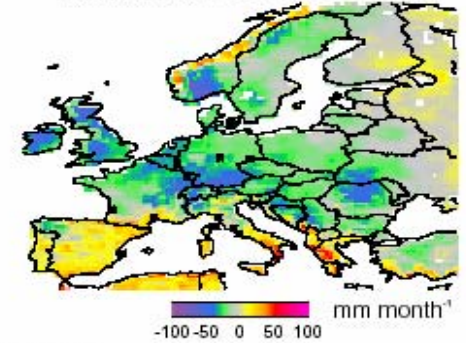
Model
verification with
EOS-MODIS
FAPAR

Climate

JUL-SEP Temperature 2003 vs 1998-2002

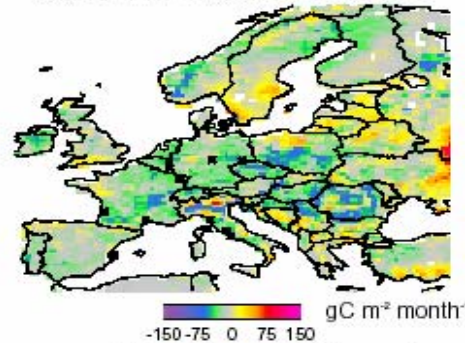


Annual Rain 2003 vs 1998-2002

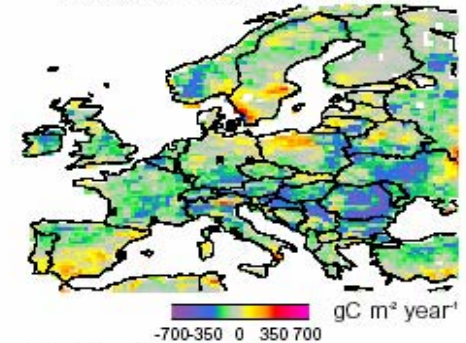


Net Primary Productivity

JUL-SEP NPP 2003 vs 1998-2002

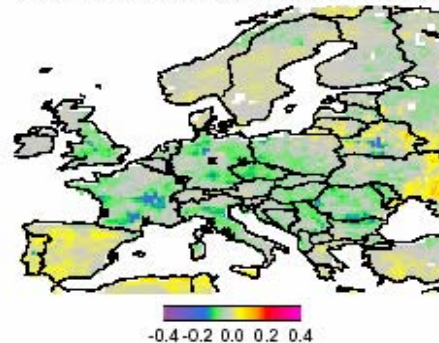


Annual NPP 2003 vs 1998-2002

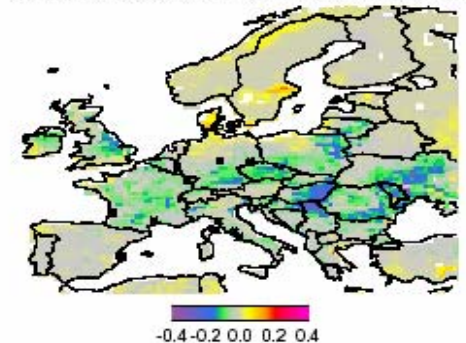


Fraction of Absorbed Photosynthetic Radiation

MODIS JUL-SEP 2003 vs 2000-2002



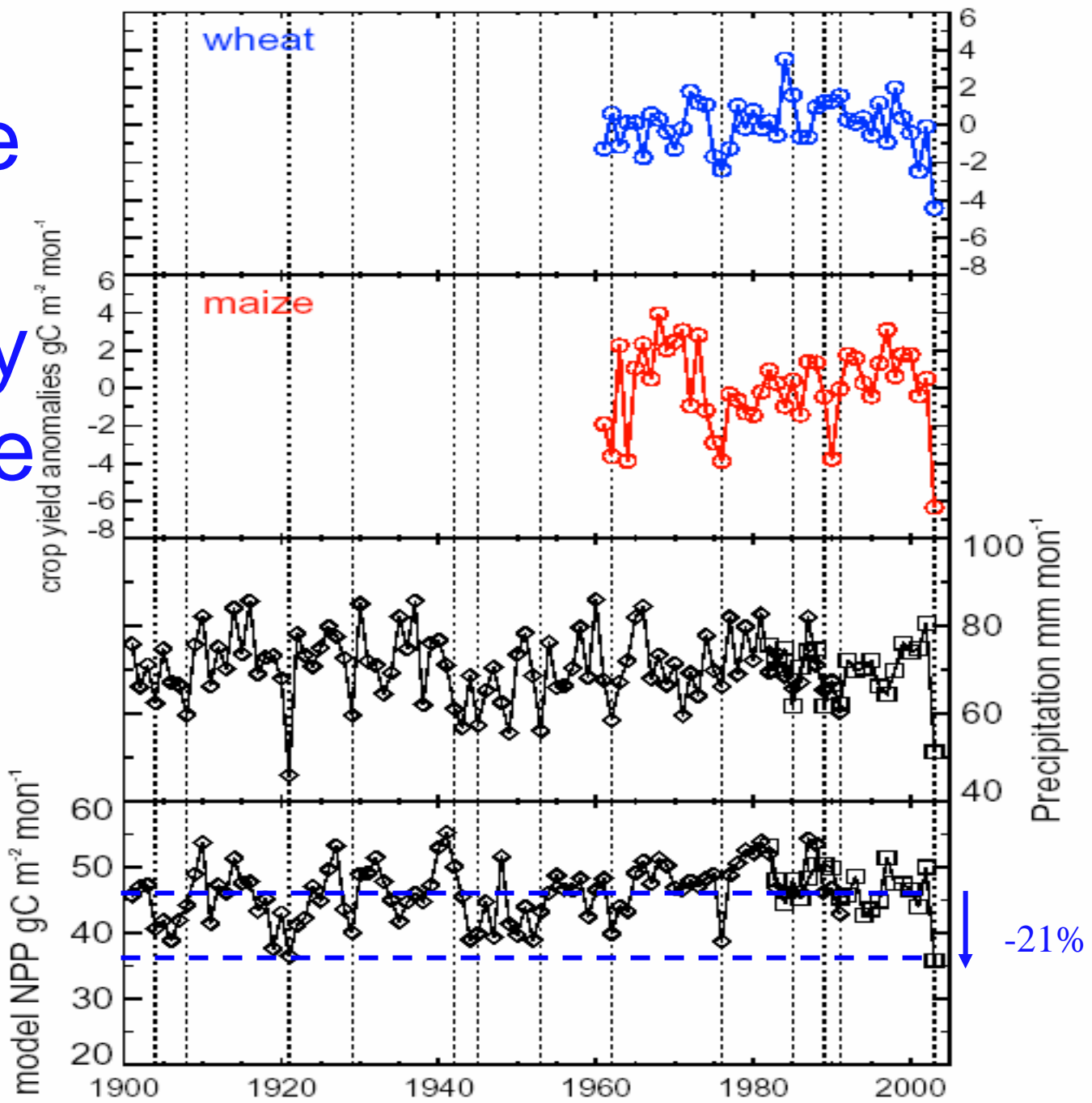
Simulated JUL-SEP 2003 vs 2000-2002



Verification against crops yield national data

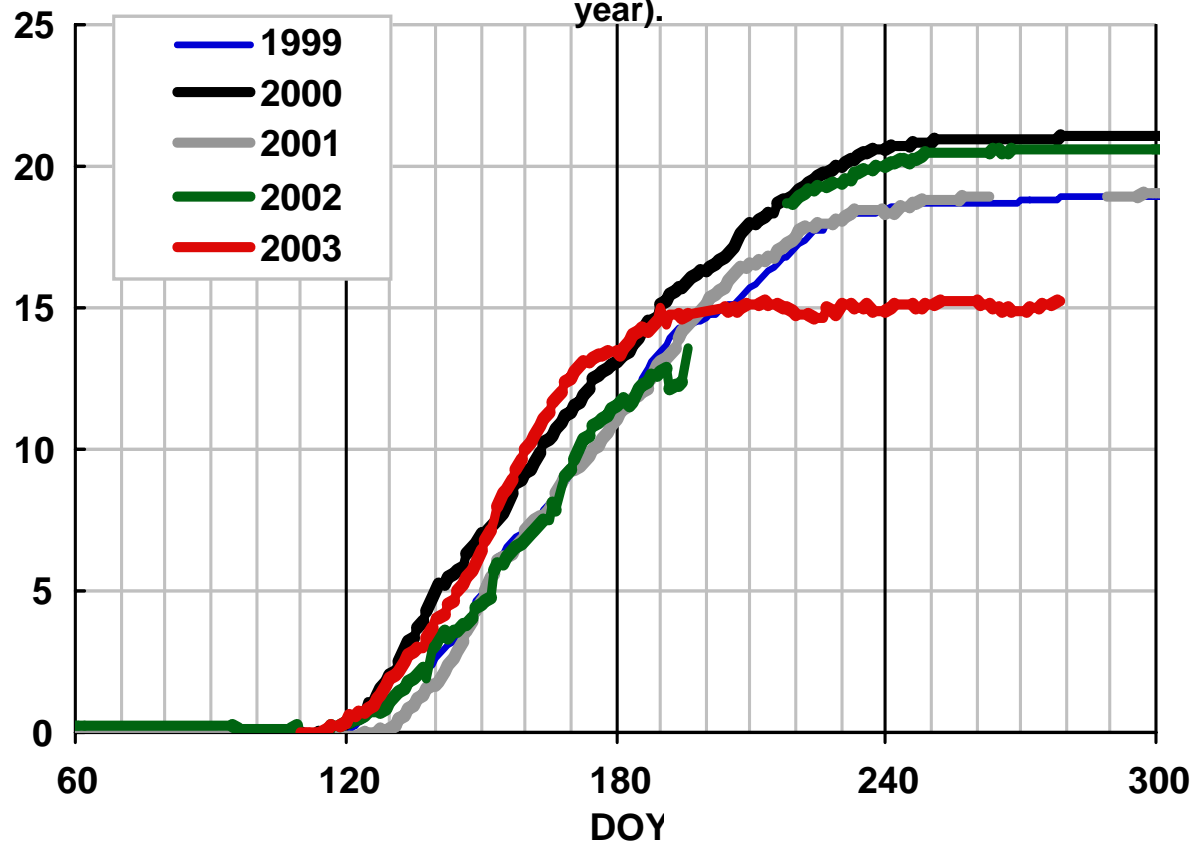
QuickTime™ et un
décompresseur TIFF (LZW)
sont requis pour visionner cette image.

2003 is the largest productivity crash of the past 100 years



Independent tree ring verification

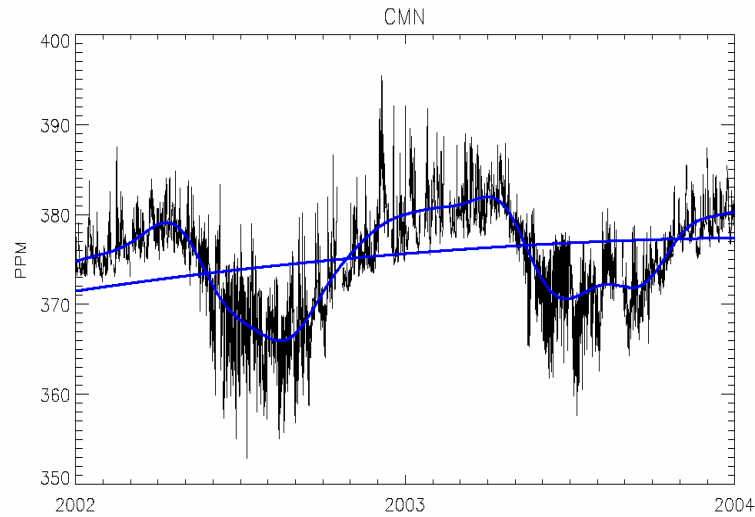
Hesse: seasonal variation of tree circumference as measured on beech trees among the dominant and codominant crown class during the period 1999-2003 (the same trees were measured each year).



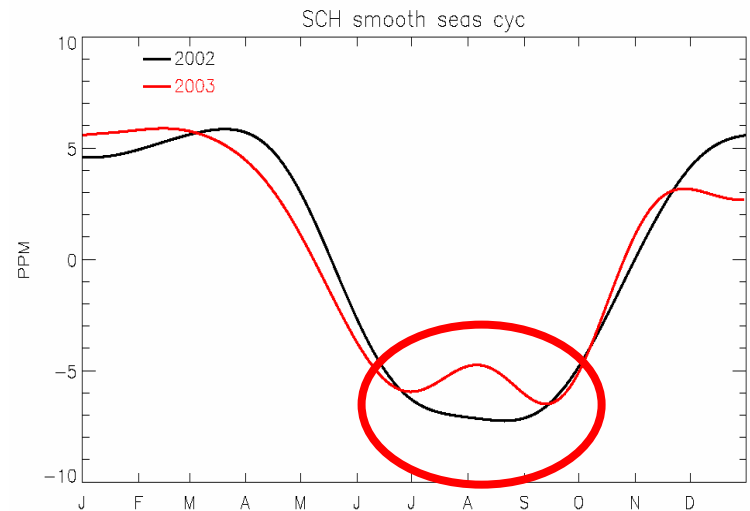
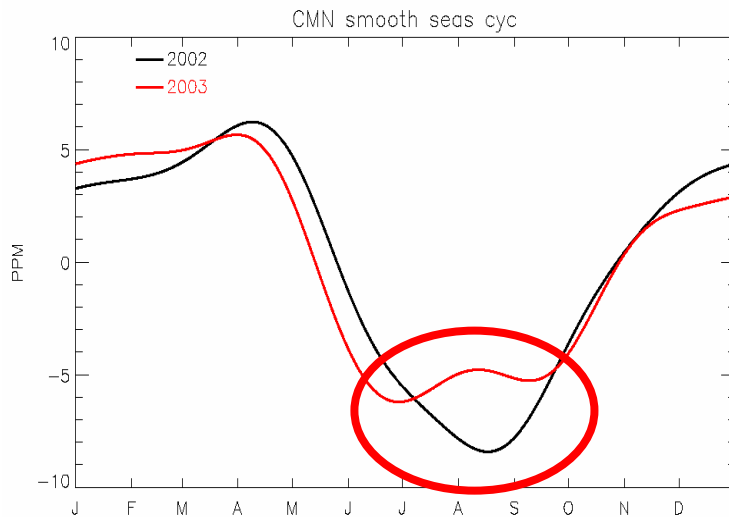
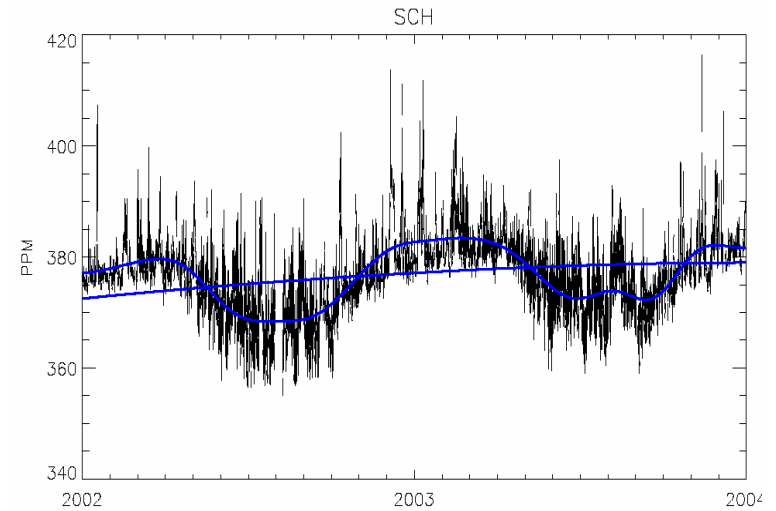
A. Granier pers. Comm

Independent Atmospheric Verification of NEE (in progress)

Monte cimone, 2100 m (Italy)



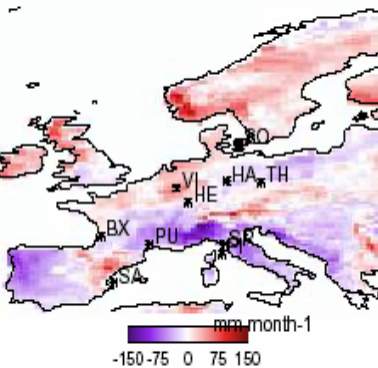
Schauinsland, 1200 m (Germany)



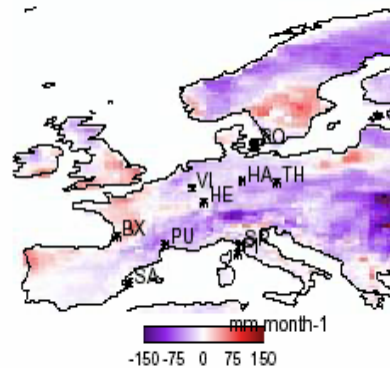
Precipitation

NPP

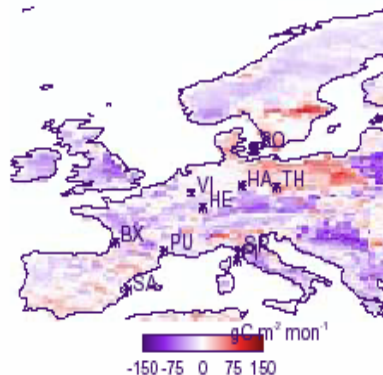
MAY 2003 vs 1998-2002



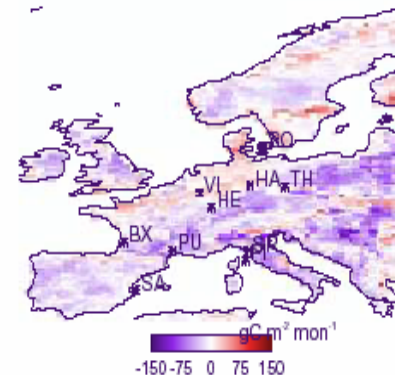
JUN 2003 vs 1998-2002



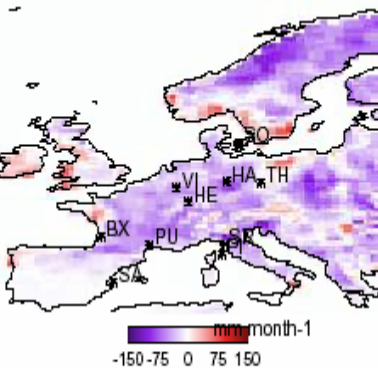
MAY 2003 vs 1998-2002



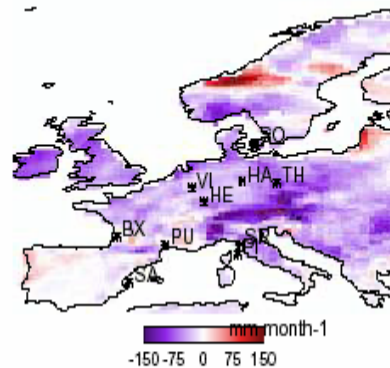
JUN 2003 vs 1998-2002



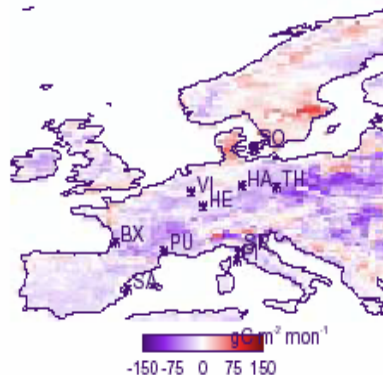
JUL 2003 vs 1998-2002



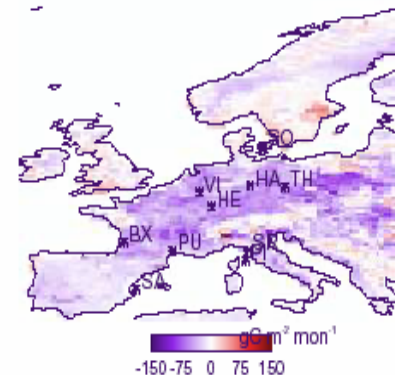
AUG 2003 vs 1998-2002



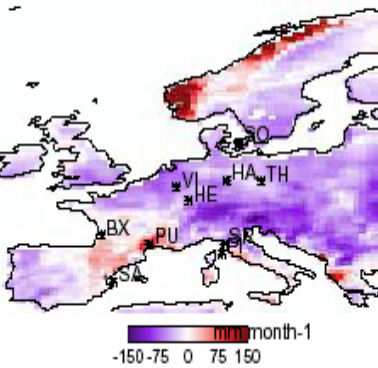
JUL 2003 vs 1998-2002



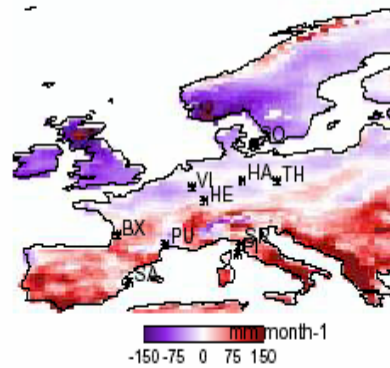
AUG 2003 vs 1998-2002



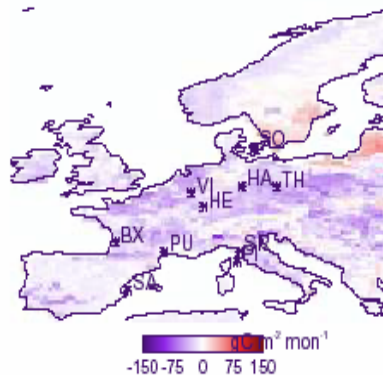
SEP 2003 vs 1998-2002



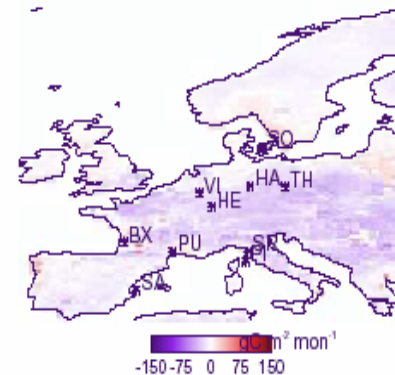
OCT 2003 vs 1998-2002



SEP 2003 vs 1998-2002



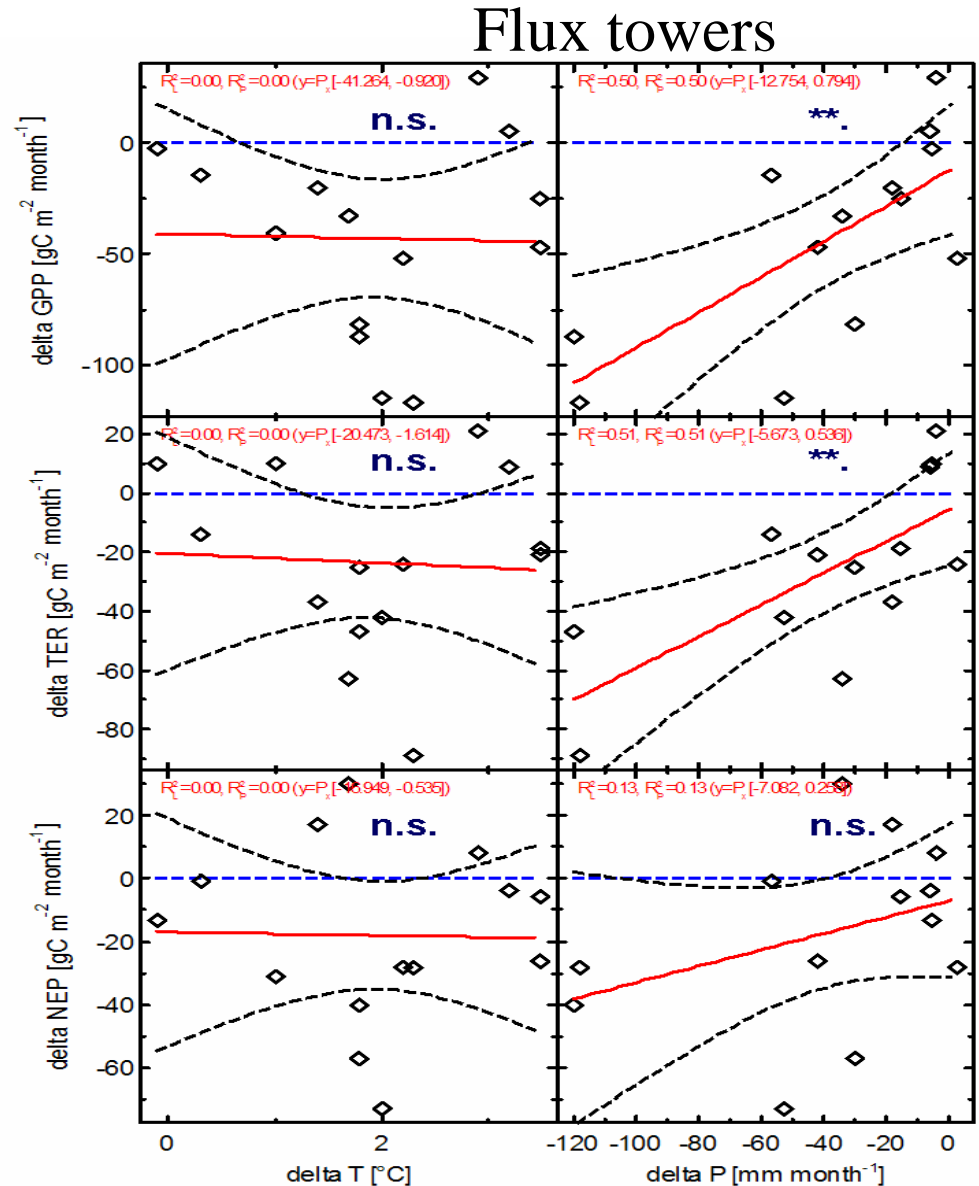
OCT 2003 vs 1998-2002

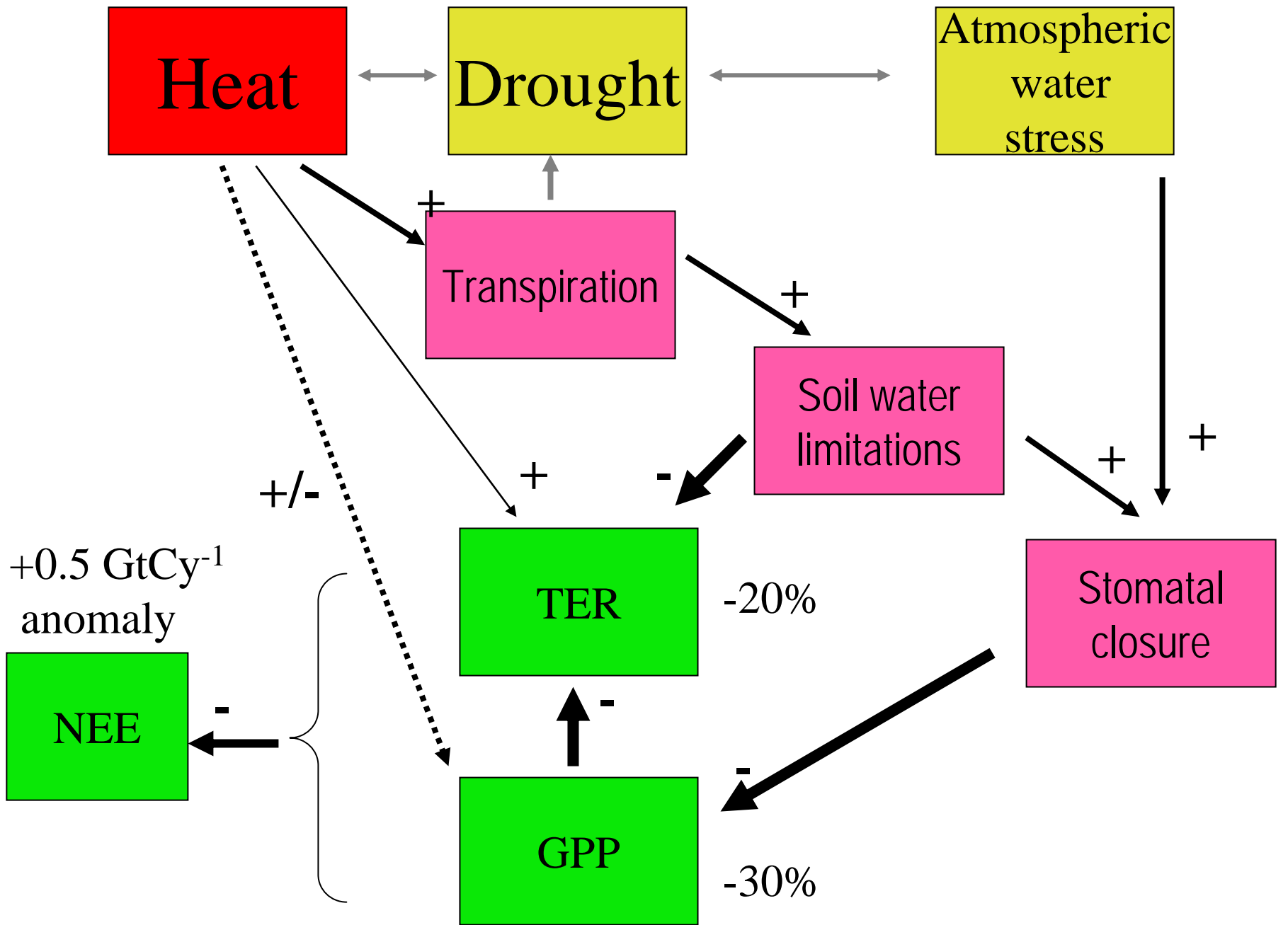


Did Rainfall deficit drives the GPP decrease ?

Model

QuickTime™ et un décompresseur TIFF (LZW) sont requis pour visionner cette image.





Soil water content variation model and observations indicate large water stress at all sites in 2003 with Root Extractable Water (REW) < 0.4

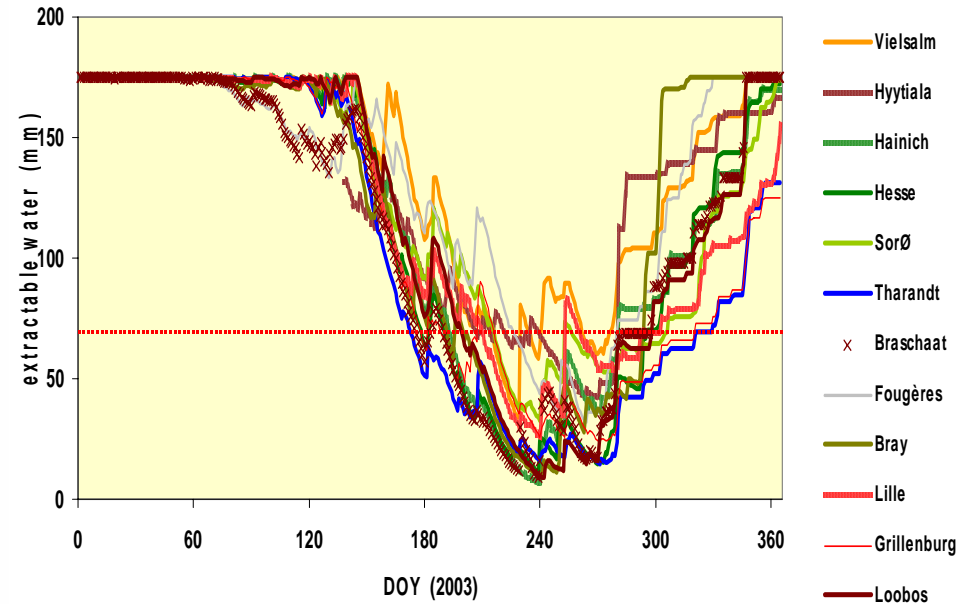
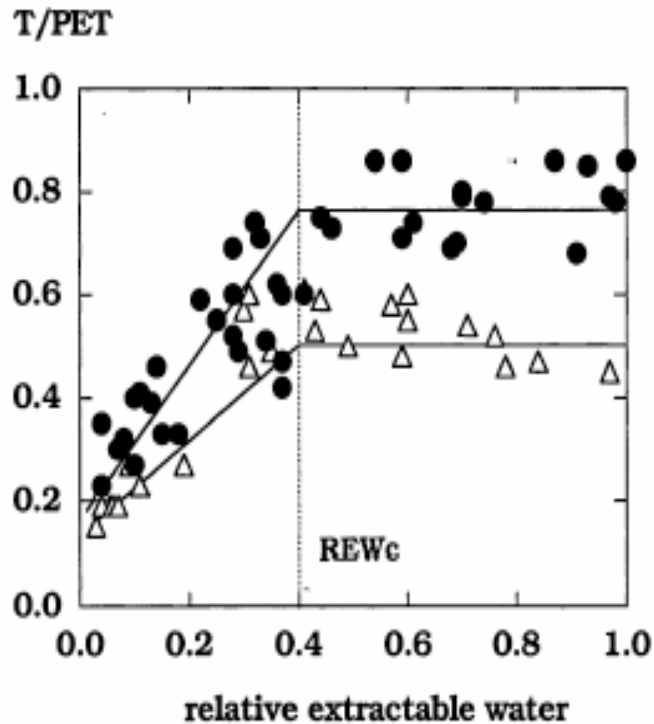
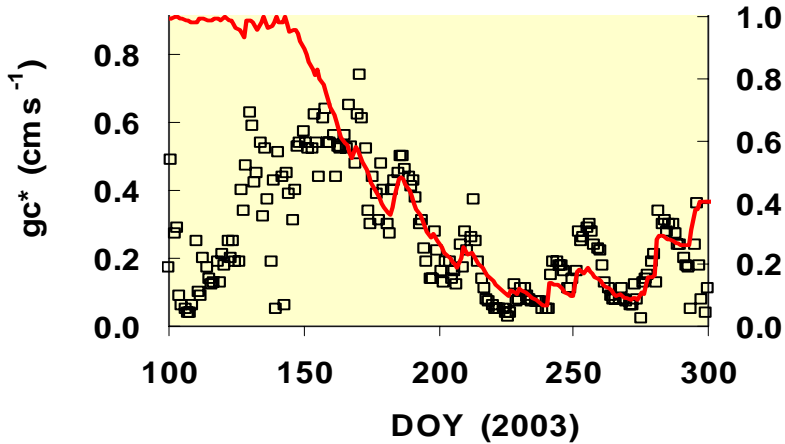


Fig. 2. Ratio T/PET calculated from sap flow measurements in an oak stand as a function of relative extractable water (REW) calculated from neutron probe measurements (from Bréda and Granier, 1996). Two data sets are reported: $LAI = 6 \text{ m}^2 \text{ m}^{-2}$ (black circles) and $LAI = 4.5 \text{ m}^2 \text{ m}^{-2}$ (open triangles). The dotted line shows the critical REW (REW_c).

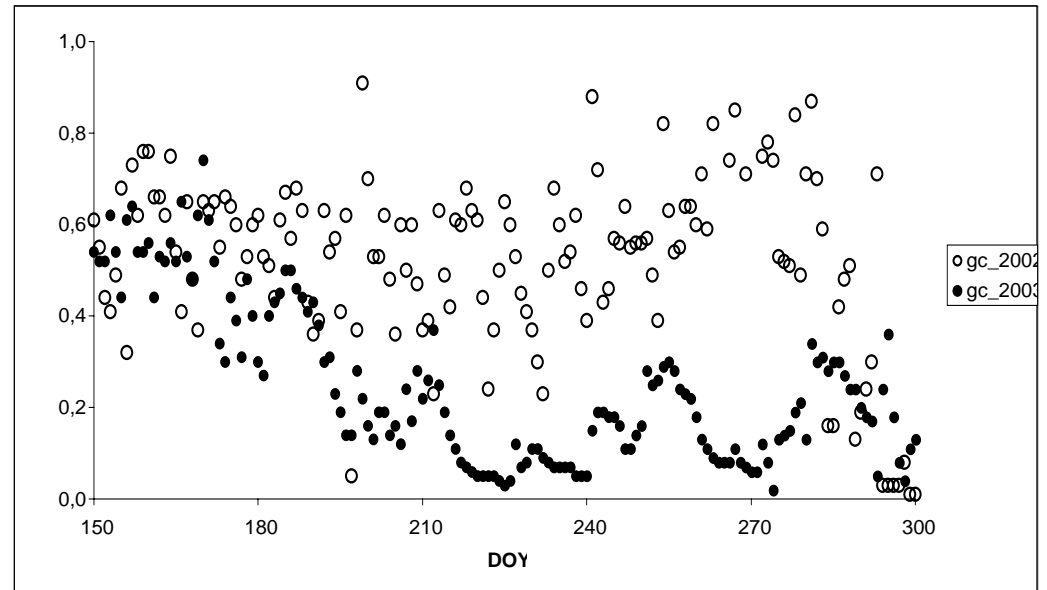
Breda et al. 1999

Granier et al. analysis confirms water-stress controls

Canopy conductance
correlates with soil water
stress



Canopy conductance in 2003 at Hesse was 15% of its 2002 value !



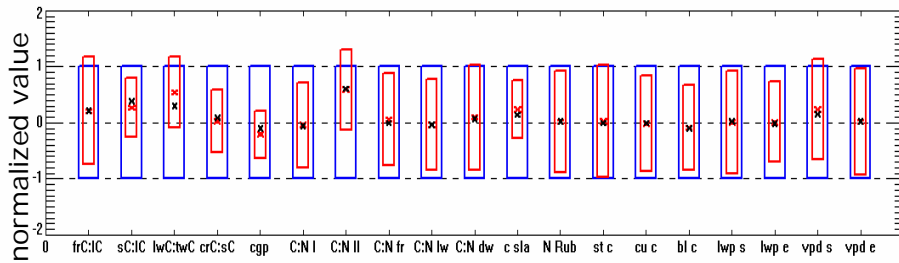
Modellers, be brave !

test your best parameters for 2003!

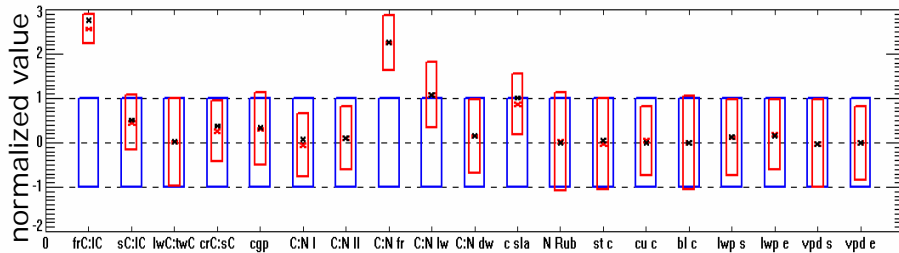
See also Wang et al. , Poster by Santaren, etc..

BIOME-BGC Model Parameters

Deciduous broadleaf forest



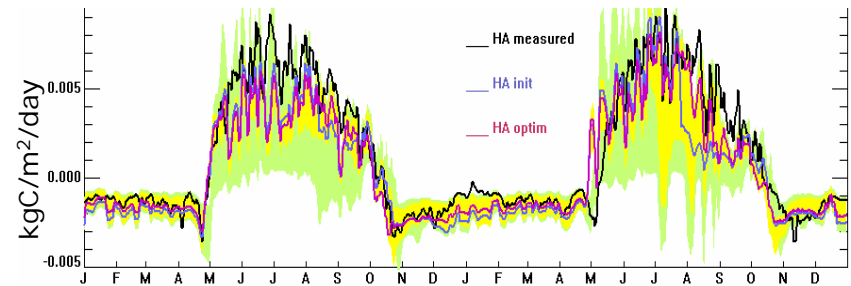
Evergreen needle leaf forest



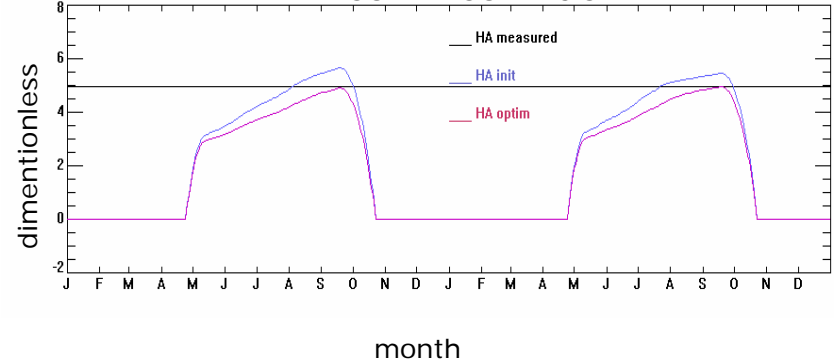
ecophysiological parameters

Parameter range before optimization
 Parameter range after optimization

Model Results NEE

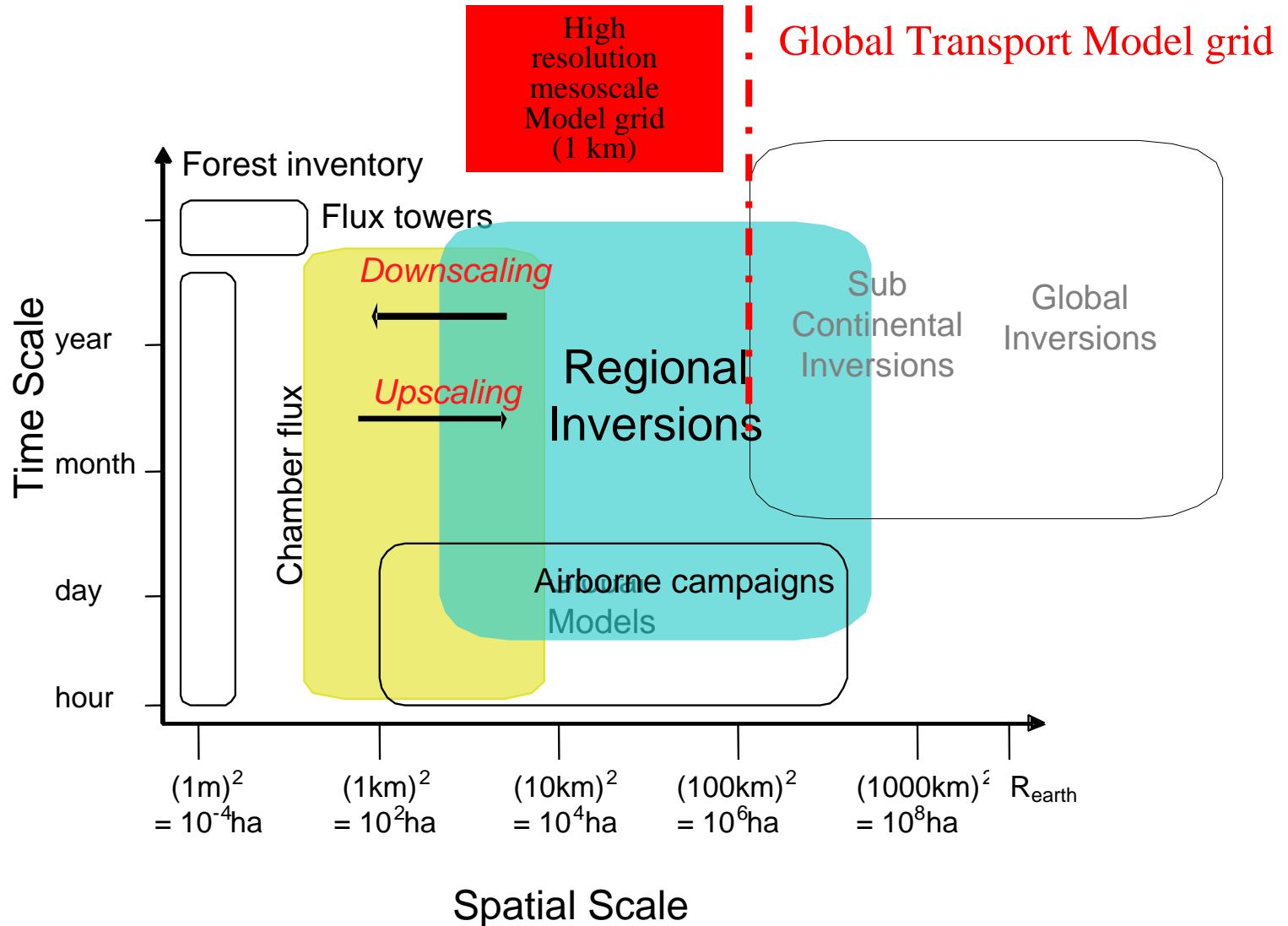


Leaf Area Index



Trusilova and Churkina
in preparation

Joint constraints! Complementary methods 3. Regional Inversions



WLEF CO₂ flux and mixing ratio observatory

K. Davis and colleagues



WLEF tall tower (447m)

CO₂ flux measurements at:

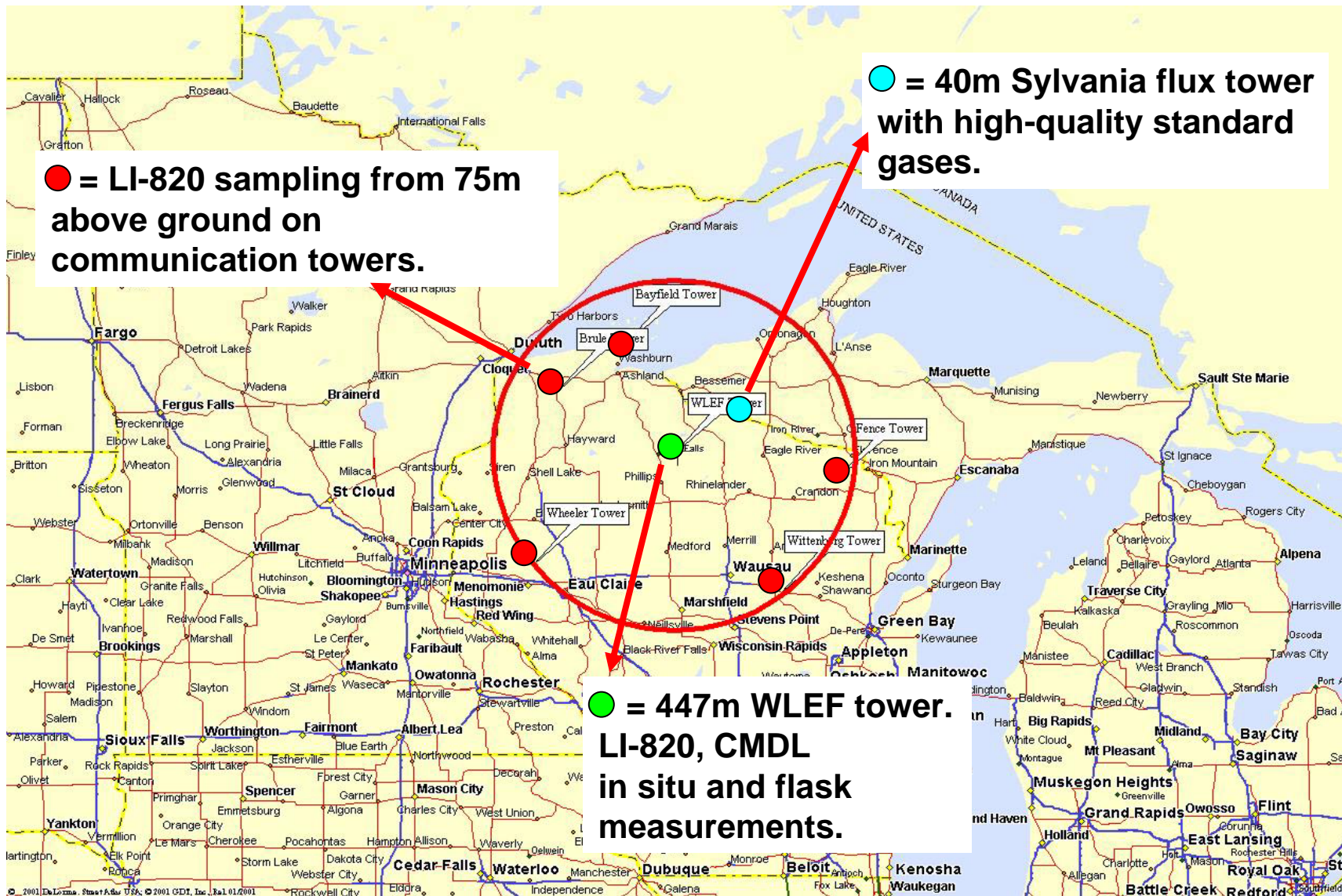
30, 122 and 396 m

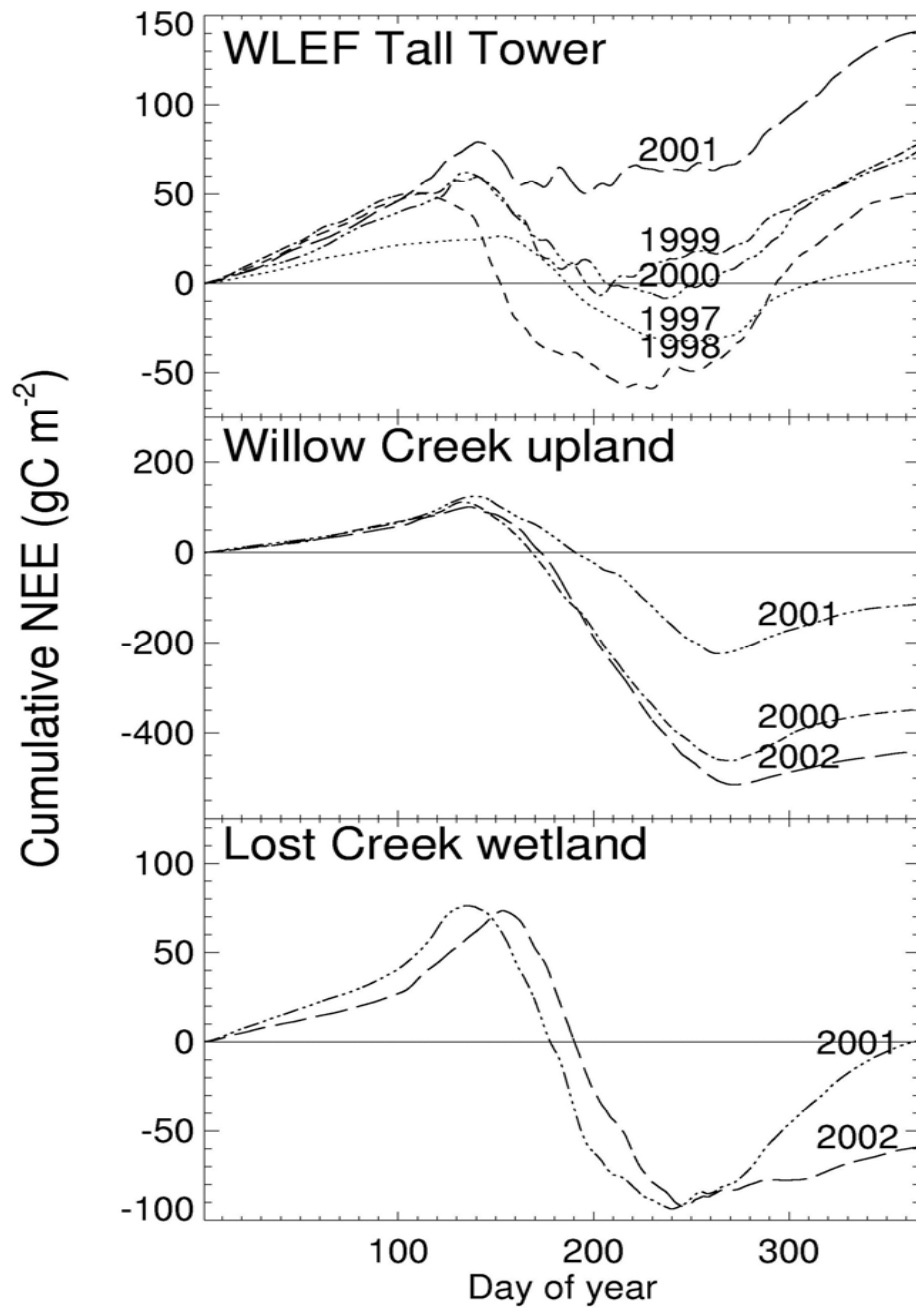
CO₂ mixing ratio measurements at:

11, 30, 76, 122, 244 and 396 m

Photo credit: UND Citation crew, COBRA

ChEAS Regional Flux Experiment Domain





NEE and gross fluxes at ChEAS sites: 1997-2002

	NEE (gC m ⁻²)	Respiration (gC m ⁻²)	Photosynthesis (gC m ⁻²)
WLEF 1997	27	991	964
WLEF 1998	48	986	938
WLEF 1999	100	1054	954
WLEF 2000	74	1005	931
WLEF 2001	141	1067	926
WLEF average	78	1021	942
Willow Creek 2000	-347	762	1109
Willow Creek 2001	-108	741	849
Willow Creek 2002	-437	648	1085
Willow Creek average	-297	717	1014
Lost creek 2001	1	759	758
Lost Creek 2002	-58	631	689
Lost Creek average	-30	695	724

ChEAS Regional Flux Experiment

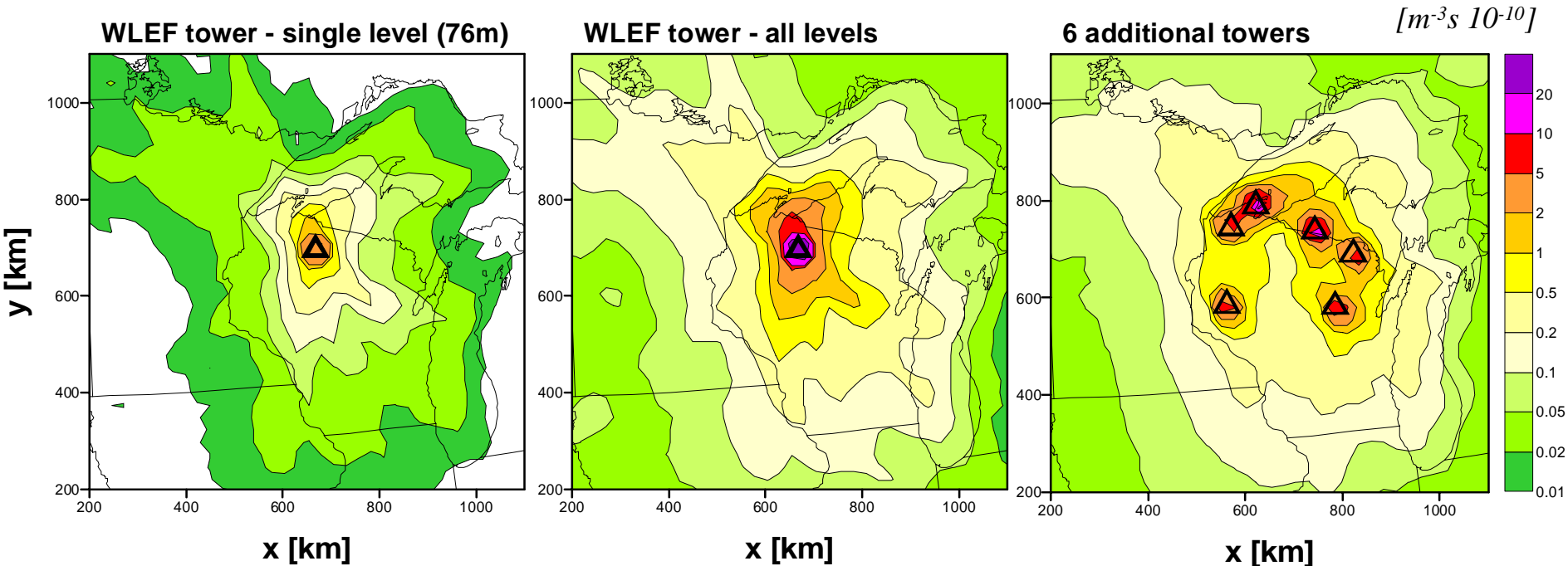
- Derive daytime and daily seasonal fluxes using regional atmospheric inversions and relatively inexpensive in situ CO₂ sensors.
- Overarching goal – evaluate/merge multiple approaches of studying terrestrial fluxes of CO₂.
 - Merge flux-tower based upscaling with downscaled inversion methodology. Regional integration and mechanistic interpretation.
 - Determine interannual variations in seasonal fluxes on a regional basis. Again, integrate with regional flux measurements/mechanistic interpretations.
 - If possible, derive net annual fluxes. Spatial resolution is limited by the magnitude of the annual signal.

Expected Regional Mixing Ratio Differences (Winter to Summer)

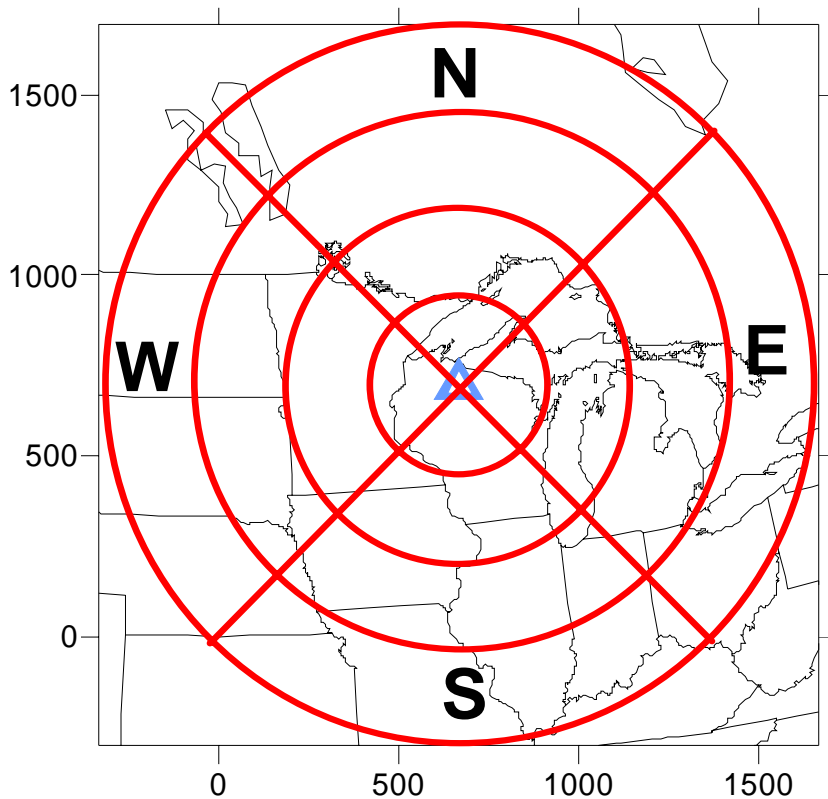
Time scale	Daytime	Diurnal	Annual
Flux magnitude	1 to 10 $\mu\text{mol m}^{-2} \text{s}^{-1}$	1 to 4 $\text{gC m}^{-2} \text{d}^{-1}$	~ 1 $\text{gC m}^{-2} \text{d}^{-1}$
Mixing depth	1 to 2 km	1 to 2 km	~ 10 km
Advection time	~ 10 hours	~ 24 hours	
Advection distance	~ 180 km (half ring)	~ 400 km (full ring)	400 km (full ring)
Change in ABL CO_2	1 to 5 ppm	2 to 5 ppm	~ 0.2 ppm

Climatology of influence functions for August 2000

- influence functions derived from RAMS/LPD model simulations
- passive tracer
- different configurations of concentration samples - time series from
 - a single level of WLEF tower
 - all levels of WLEF tower
 - six additional towers



Regional Inversions



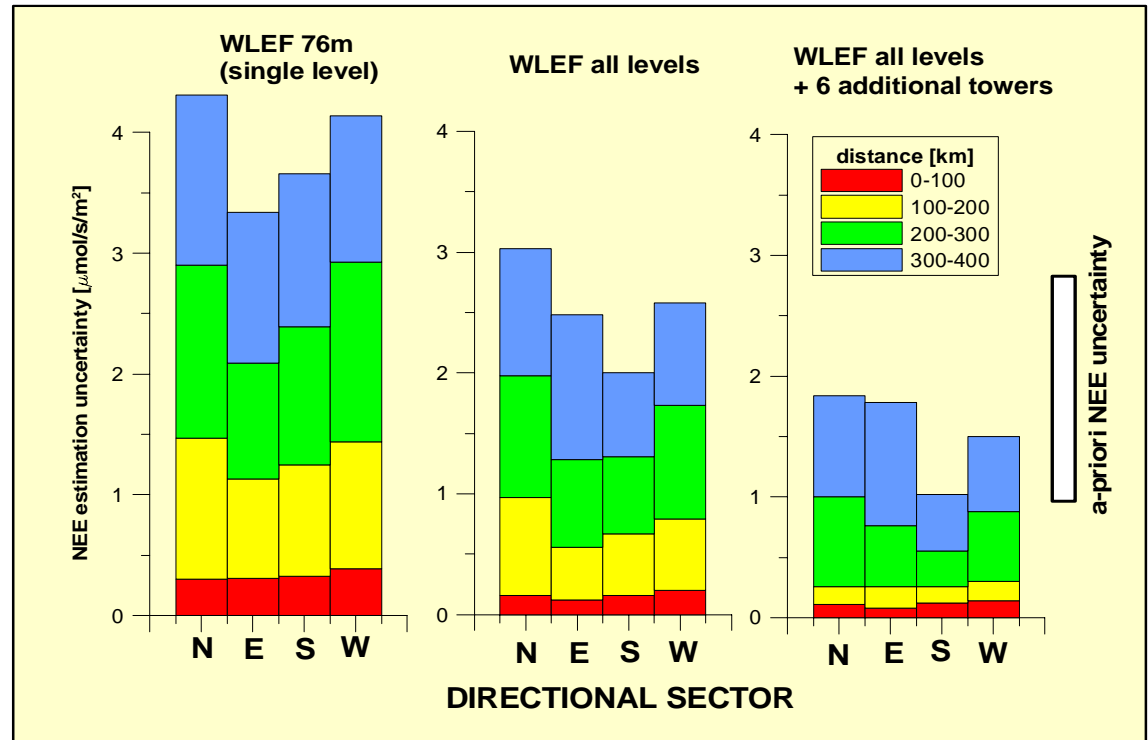
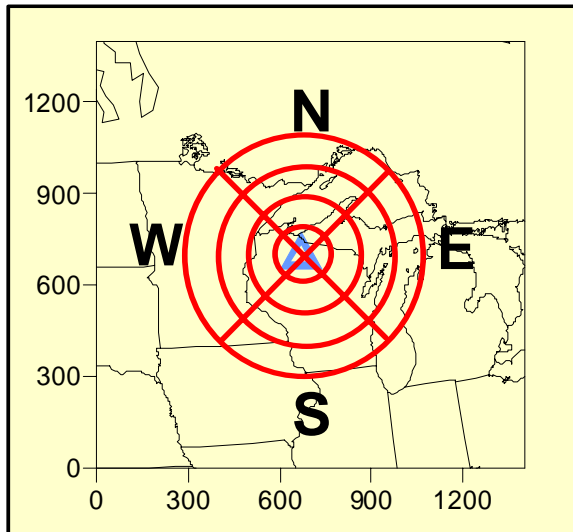
Separate estimation of
 $A(\text{PAR})$, $R(\text{T})$, FF

- Bayesian inversion technique
- source areas defined in polar coordinates centered at the WLEF tower
 - a better coverage by atmospheric transport
- [RAMS -> LPD] long term simulations
 - derivation of influence functions for concentration samples
- data: concentration time series from the WLEF tower and additional towers
- CO_2 flux decomposed into respiration and assimilation fluxes
- CO_2 inflow fluxes from a larger scale model
 - a priori estimations to be improved in inversion calculations

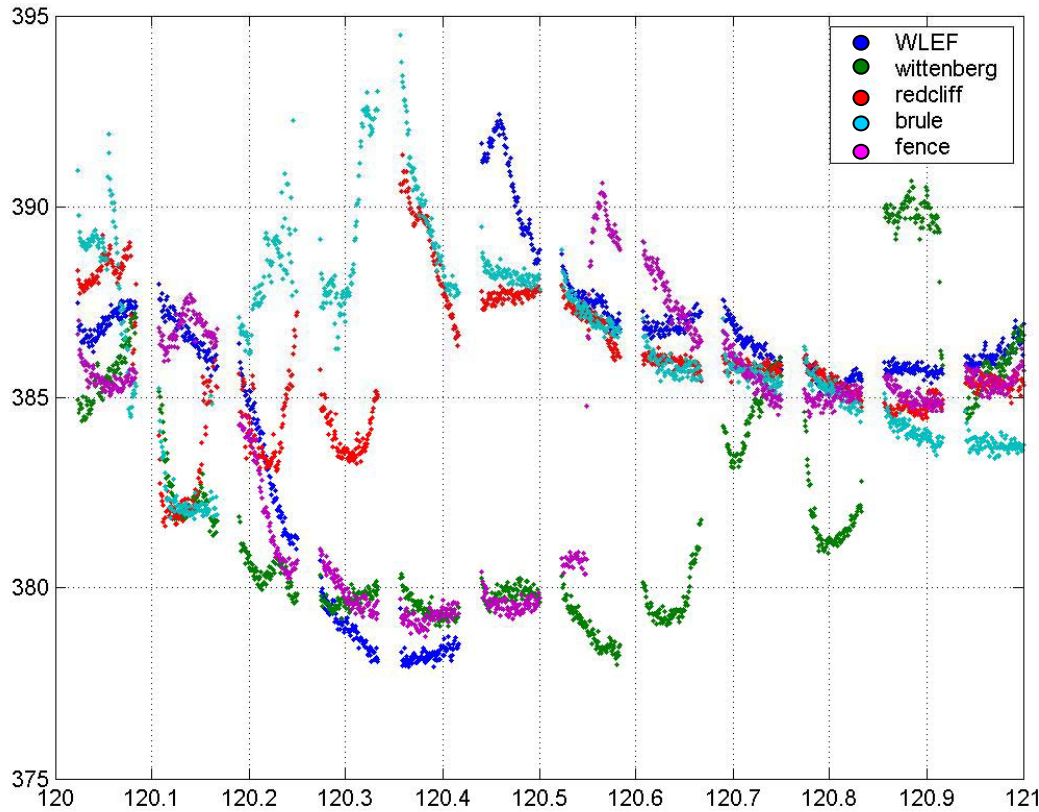
Example of estimation of NEE averaged for August 2000

- ✓ Inversion calculations for increasing number of concentration data (time series from towers)
- ✓ NEE uncertainty presented in terms of standard deviation derived from posteriori covariance matrix
- ✓ Inflow CO₂ flux is assumed to be known from a large scale transport model

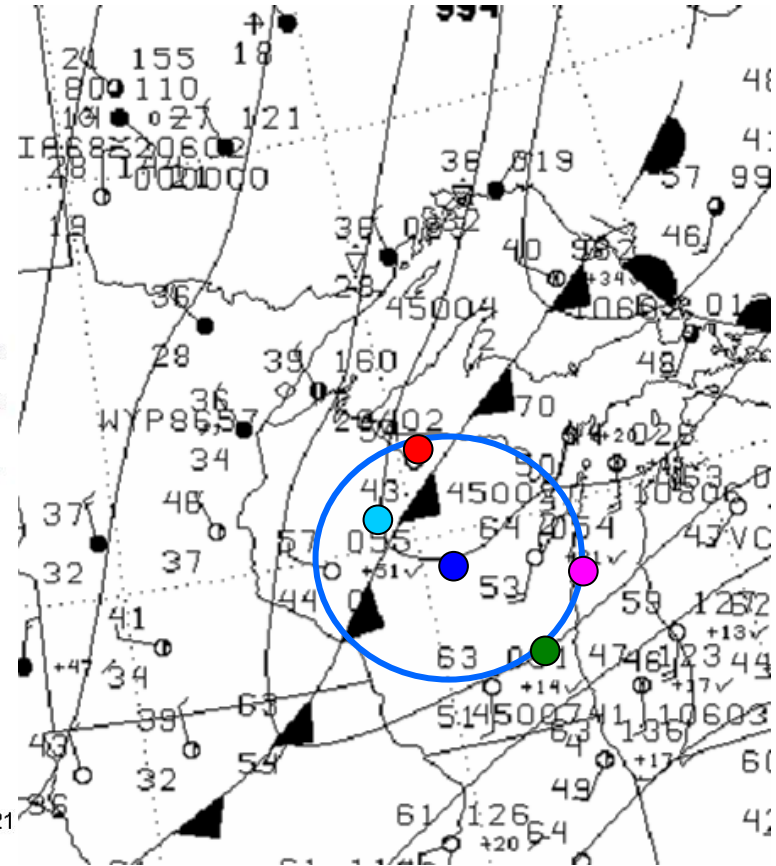
Configuration of source areas with WLEF tower in the center of polar coordinates



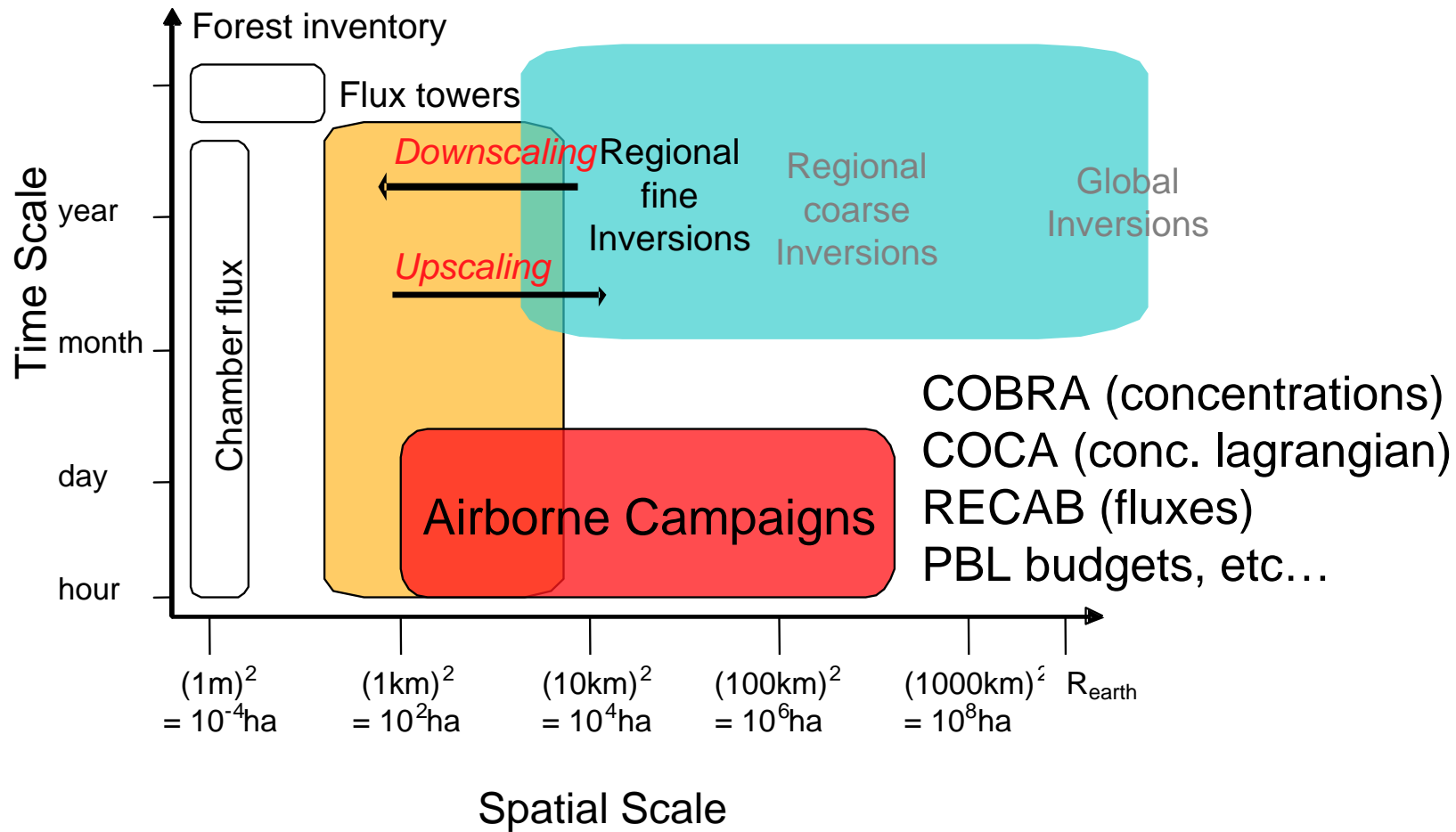
CO2 from 5 sites, April 29, 2004



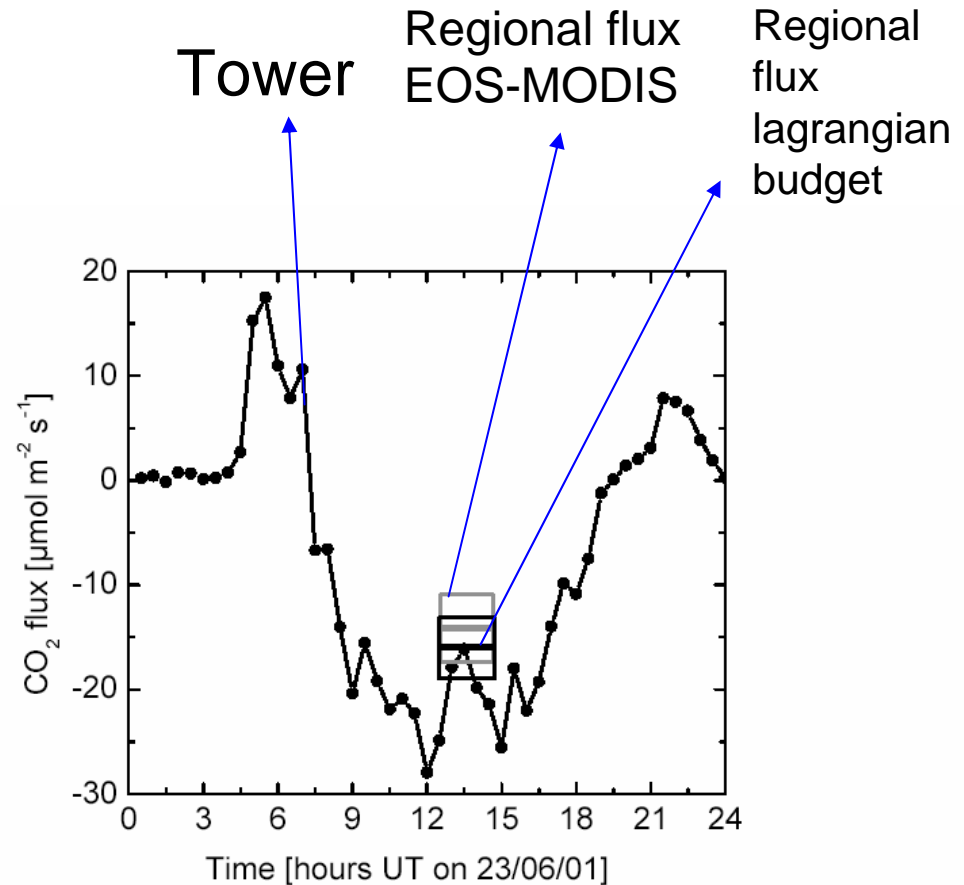
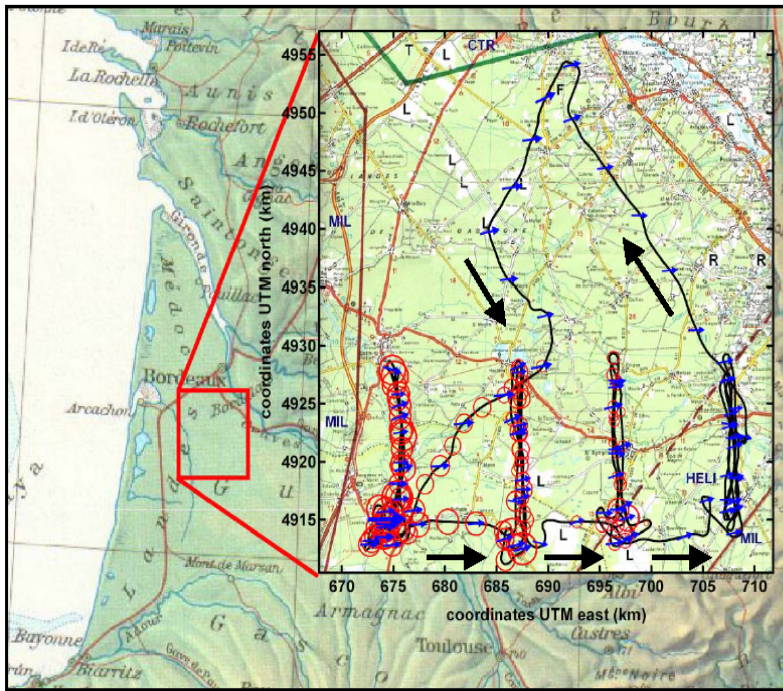
1200 UTC April 29, 2004



Joint constraints! Complementary methods : Airborne campaigns

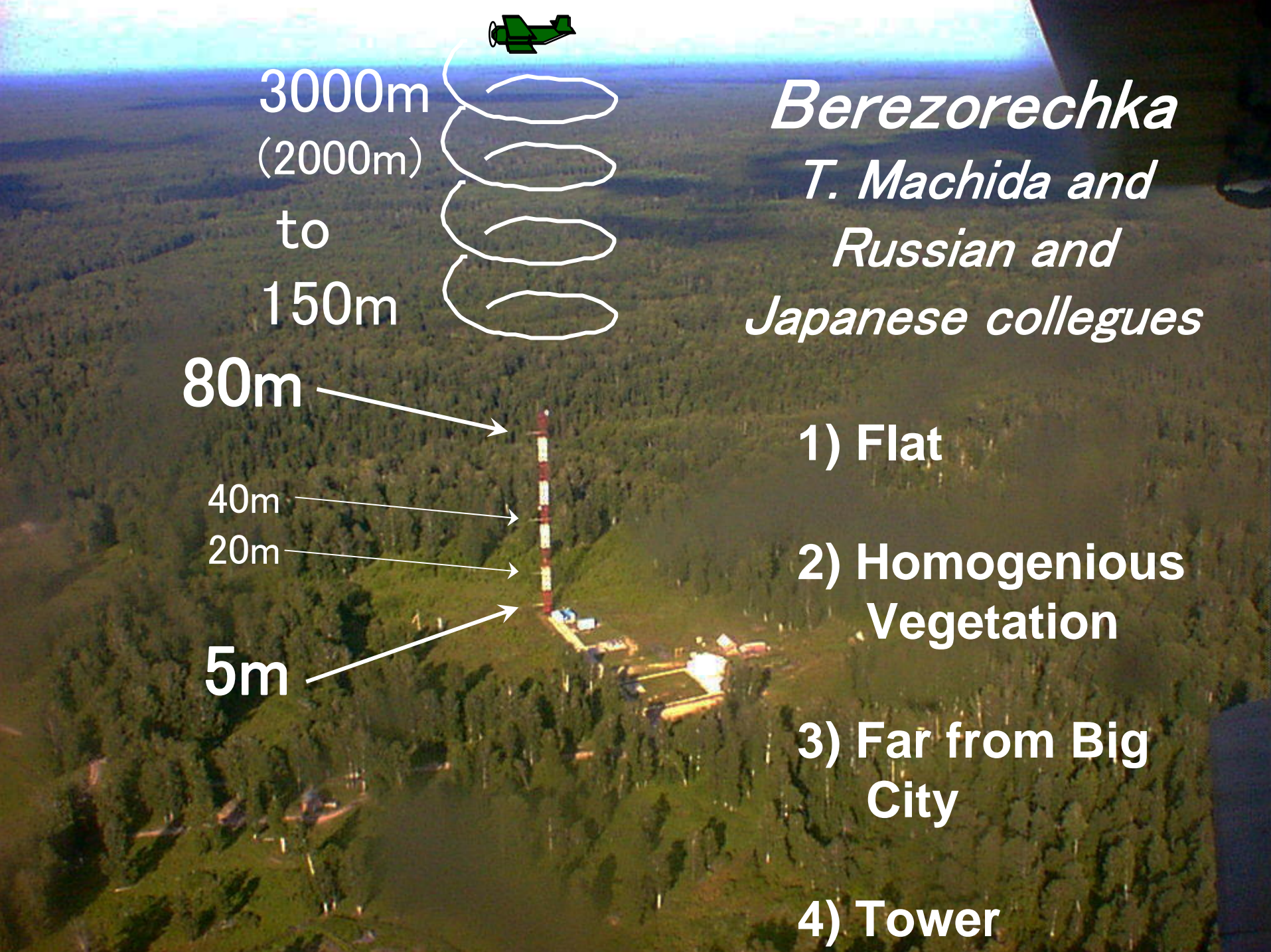


Atmospheric and bottom-up regional fluxes in Les landes



Schmitgen et al. 2004

Figure 7: Net ecosystem CO₂ exchange (NEE) from the eddy correlation measurement at the “Le Bray” tower on 23.06.2001 (circles). The black bar shows the regional NEE from the Lagrangian CBL budget, the gray bar the regional NEE modeled via remote sensing input (the boxes indicate the 1-sigma uncertainties as in Table 4).



3000m
(2000m)
to
150m



80m

40m

20m

5m

Berezorechka
T. Machida and
Russian and
Japanese colleagues

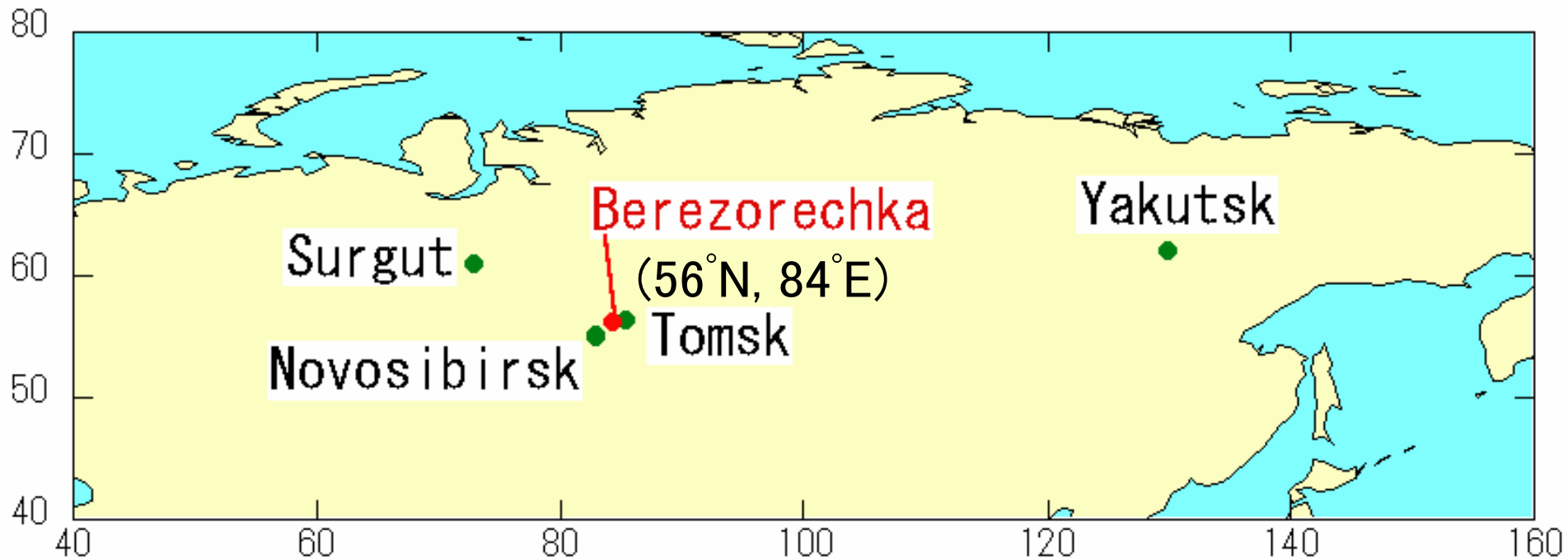
1) Flat

2) Homogenous
Vegetation

3) Far from Big
City

4) Tower

Berezorechka village, West Siberia



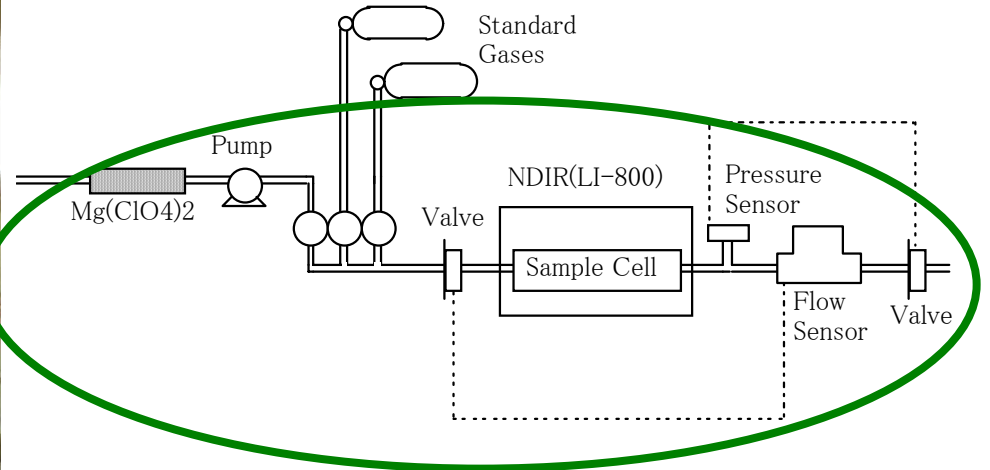


CO2 Measurement System by Air

Small Automatic

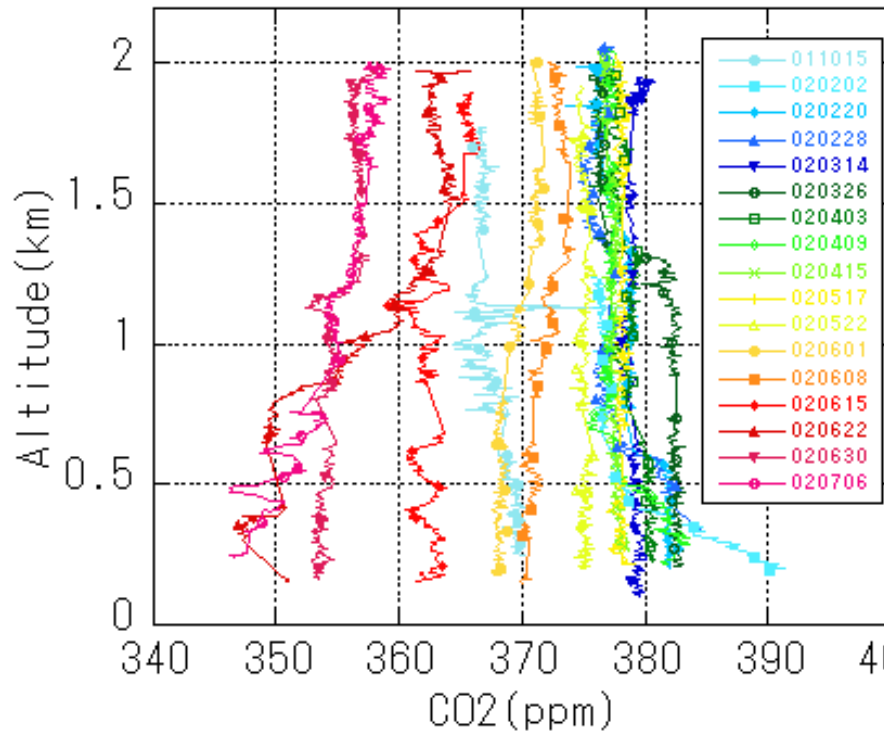


High-Frequency Measurement

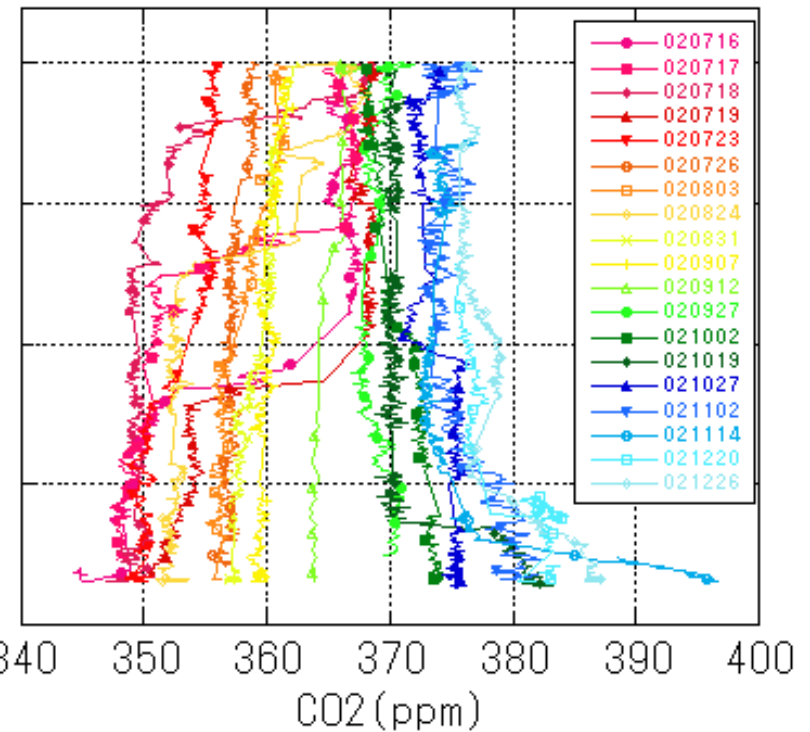


Vertical CO2 profiles in 2002

Oct.'01-Jul.'02



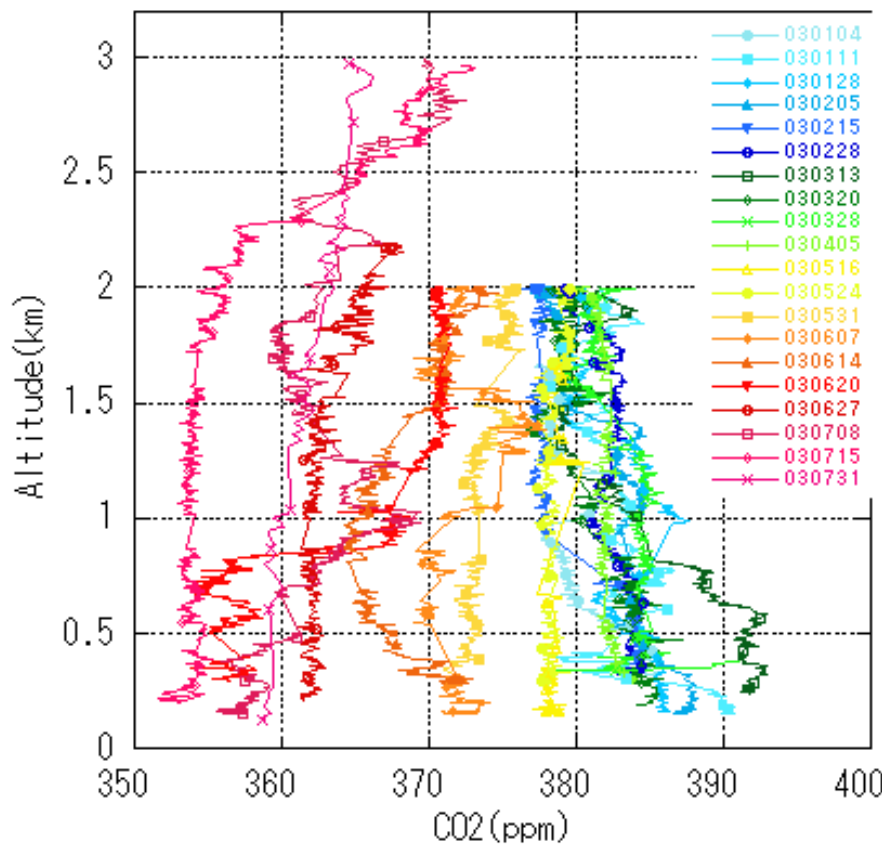
Jul.'02-Dec.'02



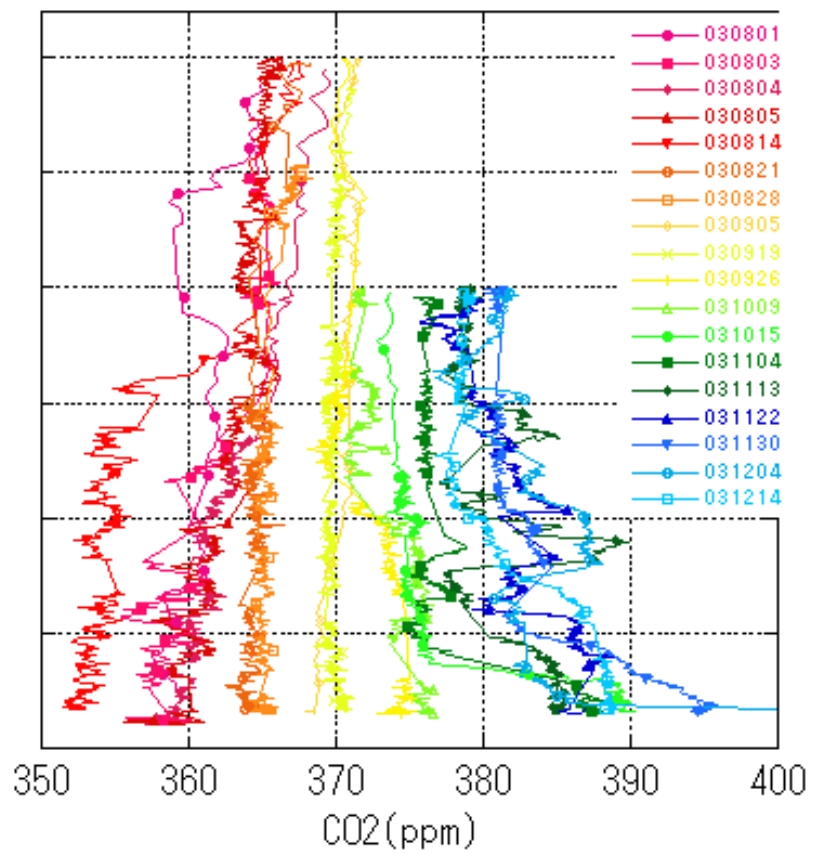
35 Flights in 2002

Vertical CO₂ profiles in 2003

Jan.'03-Jul.'03



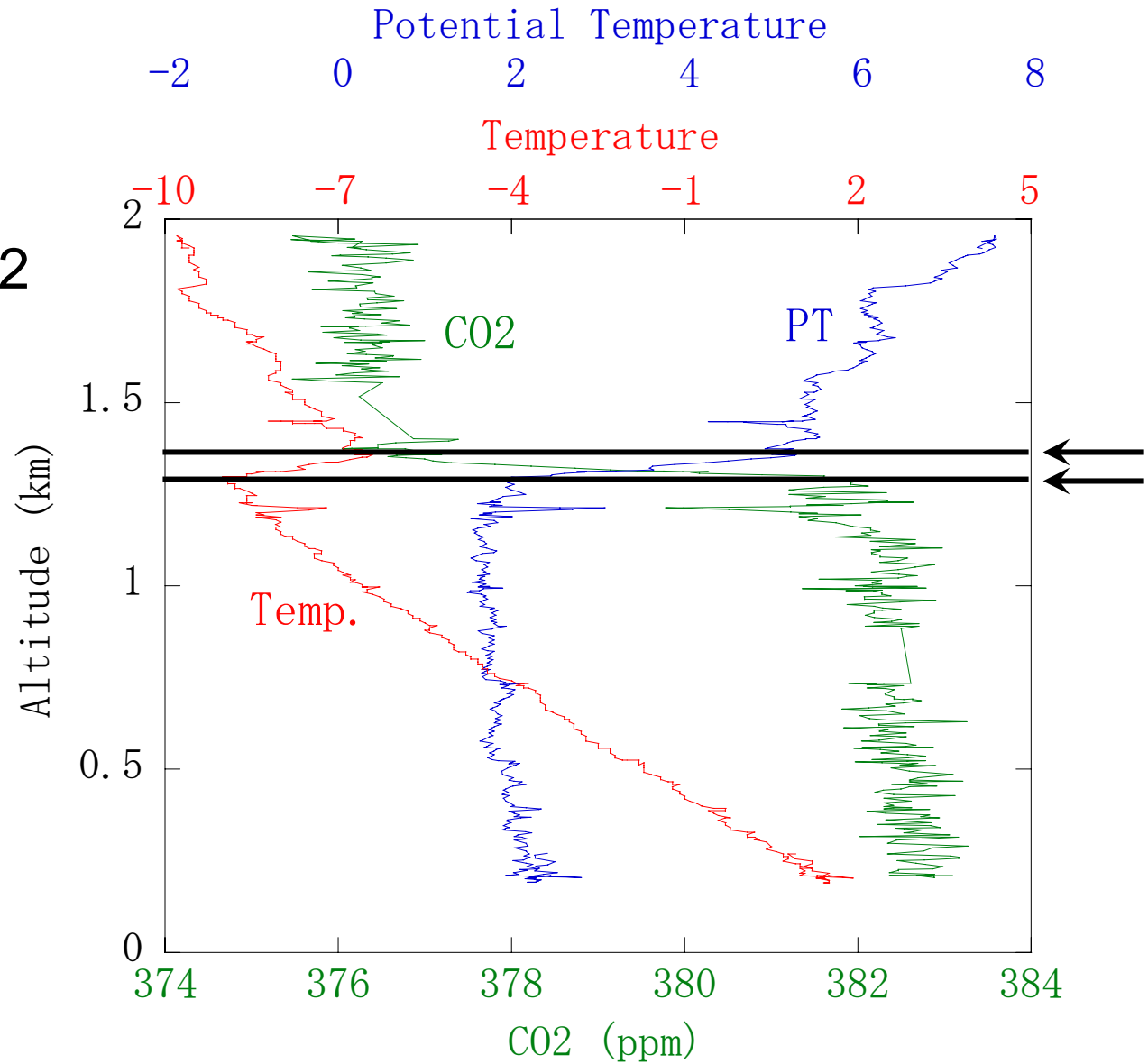
Jul.'03-Dec.'03



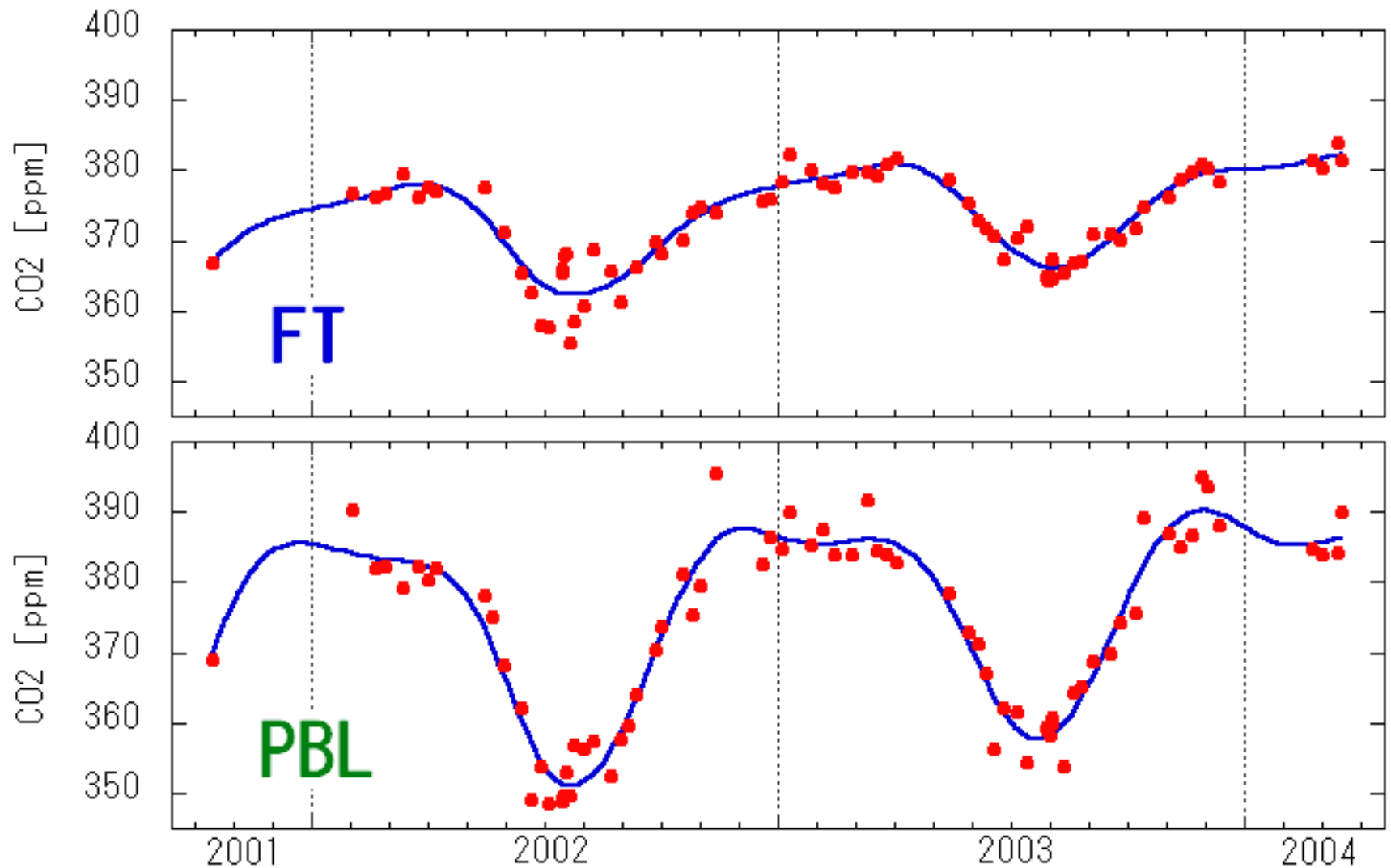
38 Flights in 2003

FT and PBL

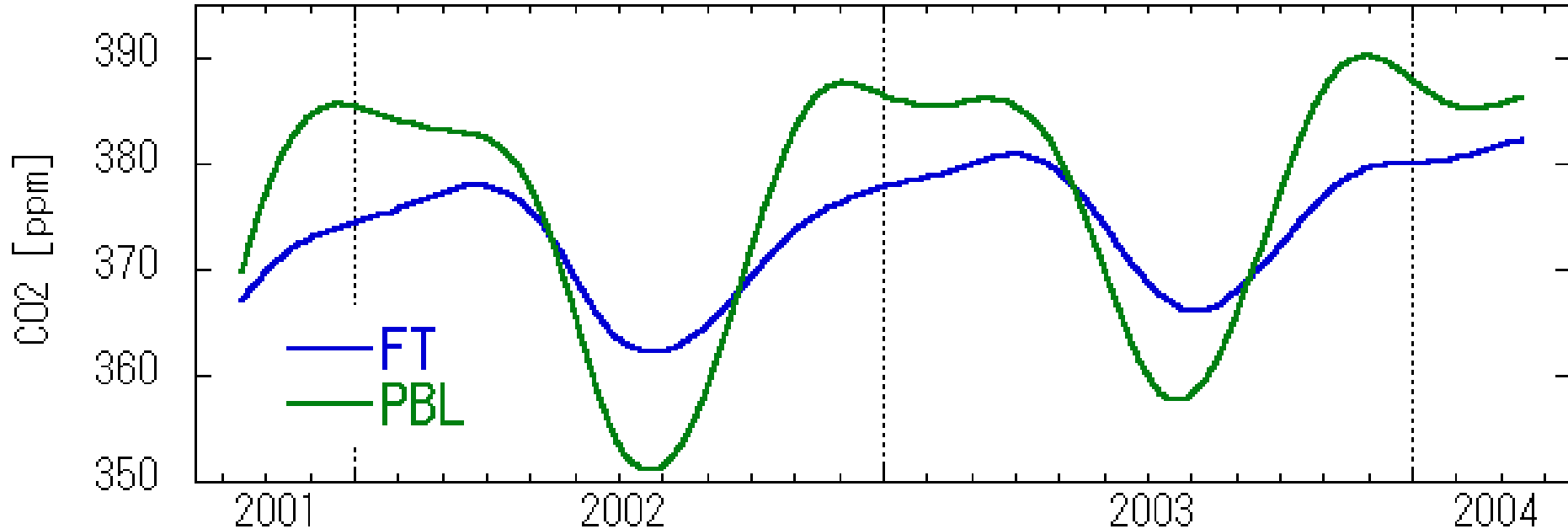
26 Mar. 2002



Temporal Variation of CO₂ in FT and PBL



Comparison of Fitting Curves

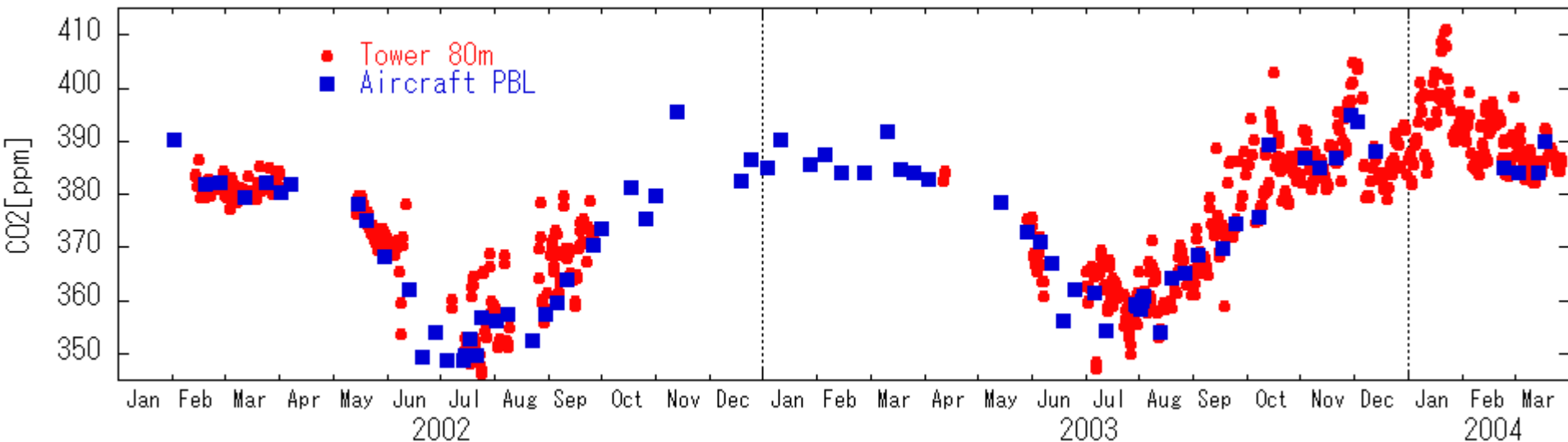


Amplitude = 16ppm(FT) and 34ppm(PBL)

High concentration in Winter

Annual average in PBL is 2ppm higher (rectifier effect)

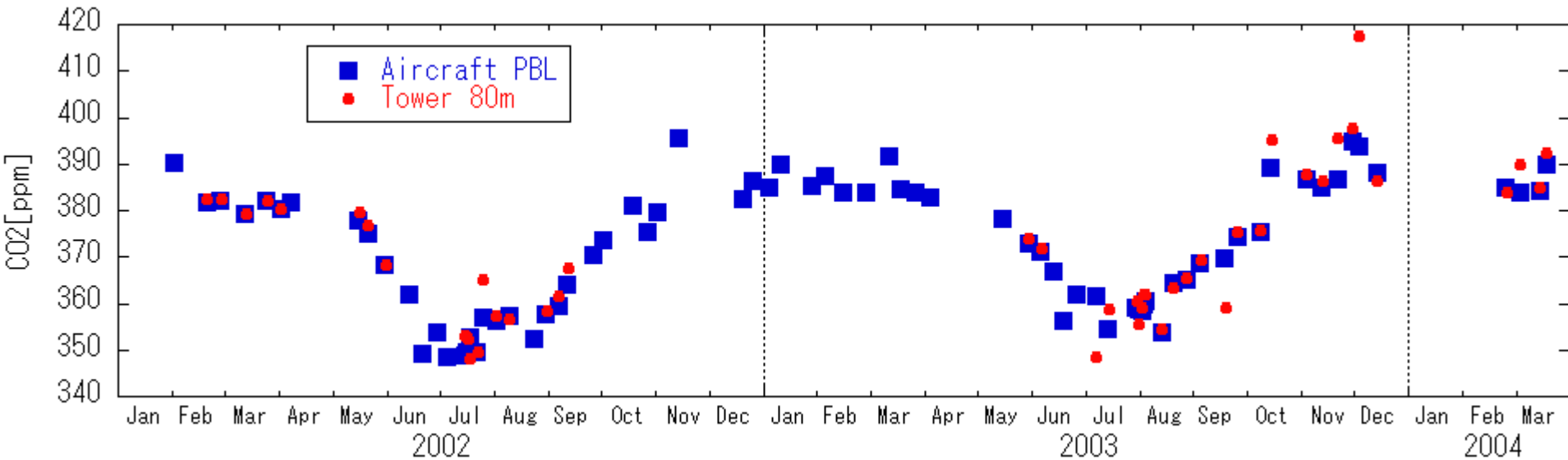
Comparison between Tower and Aircraft PBL



Substantial Difference

--> Aircraft conducts only in the good weather
Weather Bias

Comparison on the good weather condition



60% data are ± 2 ppm

Without Daytime Inversion (Winter)
No Variable day (Summer)

Conclusions

Reconciling orthogonal perspectives

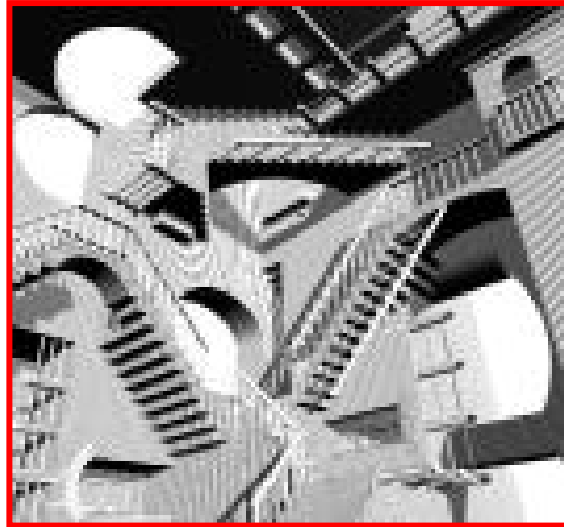
Inversion downscaling

Excellent spatial integration

Strong constraint on flux magnitude

Poor temporal resolution

Limited mechanistic understanding.



Flux tower upscaling

Intrinsically local measurements.

Difficult to upscale flux magnitudes. Variability easier

Excellent temporal resolution

Strong mechanistic understanding

Let's fusion flux upscaling and Inversions !!!

CCDAS,

Coupling of energy budget parameters with transport

Coupling of soil respiration to atmosphere